

The Nucleus-Encoded *trans*-Acting Factor MCA1 Plays a Critical Role in the Regulation of Cytochrome *f* Synthesis in *Chlamydomonas* Chloroplasts ^{IV}

Alix Boulouis, Cécile Raynaud,¹ Sandrine Bujaldon, Aude Aznar, Francis-André Wollman, and Yves Choquet²

Unité Mixte de Recherche 7141, Centre National de la Recherche Scientifique/Université Pierre et Marie Curie, Institut de Biologie Physico-Chimique, F-75005 Paris, France

Organelle gene expression is characterized by nucleus-encoded *trans*-acting factors that control posttranscriptional steps in a gene-specific manner. As a typical example, in *Chlamydomonas reinhardtii*, expression of the chloroplast *petA* gene encoding cytochrome *f*, a major subunit of the cytochrome *b₆f* complex, depends on MCA1 and TCA1, required for the accumulation and translation of the *petA* mRNA. Here, we show that these two proteins associate in high molecular mass complexes that also contain the *petA* mRNA. We demonstrate that MCA1 is degraded upon interaction with unassembled cytochrome *f* that transiently accumulates during the biogenesis of the cytochrome *b₆f* complex. Strikingly, this interaction relies on the very same residues that form the repressor motif involved in the Control by Epistasy of cytochrome *f* Synthesis (CES), a negative feedback mechanism that downregulates cytochrome *f* synthesis when its assembly within the cytochrome *b₆f* complex is compromised. Based on these new findings, we present a revised picture for the CES regulation of *petA* mRNA translation that involves proteolysis of the translation enhancer MCA1, triggered by its interaction with unassembled cytochrome *f*.

INTRODUCTION

In the time since endosymbiosis, most genes of the organelle ancestors have been either lost or transferred to the nucleus of the host cell (Martin et al., 1998; Timmis et al., 2004; Keeling, 2009). In the green lineage, the chloroplast genome has retained <100 protein-encoding genes, out of >3000 in its cyanobacterial progenitor. Their protein products participate mostly in photosynthesis or in the expression of the chloroplast genome (Barkan and Goldschmidt-Clermont, 2000). Mitochondrial genomes have become even smaller, retaining only 8, 13, and 8 open reading frames in the yeast *Saccharomyces cerevisiae*, in human, and in the green unicellular alga *Chlamydomonas reinhardtii*, respectively (Anderson et al., 1981; de Zamaroczy and Bernardi, 1986; Foury et al., 1998; Cardol and Remacle, 2009). Consequently, respiratory or photosynthetic protein complexes, with the exception of mitochondrial complex II, result from the stoichiometric assembly of subunits encoded in either the organellar or nuclear genomes. Thus, one expects a need for some coordination in gene expression between these distinct genetic compartments.

The stoichiometric accumulation of the various subunits of energy-transducing protein complexes in organelles relies on a

combination of regulatory mechanisms. First, most subunits from a protein complex show a concerted accumulation, such that in the absence of a major subunit; the others are either rapidly degraded or show downregulated synthesis, an assembly-dependent regulation of translation known as the CES process (for Control by Epistasy of Synthesis) (reviewed in Choquet and Wollman, 2009). Secondly, the nucleus tightly controls the expression of organelle genes via a set of *trans*-acting factors acting at the posttranscriptional level on a single (or a few) specific target mRNA(s) (Fox, 1996; Barkan and Goldschmidt-Clermont, 2000; Choquet and Wollman, 2002; Herrin and Nickelsen, 2004).

Phenotypic studies of photosynthetic or respiratory mutants provided evidence for two major classes of nucleus-encoded factors (Choquet and Wollman, 2002). M (for maturation/stability) factors are required for the stable accumulation of their target mRNA. Typical examples taken from *Chlamydomonas* studies include the MCA1, NAC2, and MBB1 factors that protect from 5' to 3' exonucleolytic degradation the transcripts of the chloroplast genes *petA* (encoding cytochrome *f* of the *b₆f* complex; Loiselay et al., 2008), *psbD* (encoding the D2 subunit of the photosystem II reaction center; Kuchka et al., 1989; Nickelsen et al., 1994), and *psbB* (encoding the PSII core antenna CP47; Monod et al., 1992; Vaistij et al., 2000a, 2000b), respectively. T factors are required for the translation of a specific transcript, as exemplified in *Chlamydomonas* by TCA1 for the *petA* transcript (Wostrikoff et al., 2001; Raynaud et al., 2007) or RBP40 for the *psbD* transcript (Schwarz et al., 2007).

Expression of these nucleus-encoded factors is critical for organelle biogenesis. Plant and algal cells defective for a chloroplast-targeted *trans*-acting factor lose their phototrophic properties, whereas mutations in mitochondrial-targeted factors

¹ Current address: Unité Mixte de Recherche 8618, Institut de Biologie des Plantes, Plateau du Moulon de l'Université Paris-Sud, Bâtiment 630, 91405 Orsay, France.

² Address correspondence to choquet@ibpc.fr.

The author responsible for distribution of materials integral to the findings presented in this article in accordance with the policy described in the Instructions for Authors (www.plantcell.org) is: Yves Choquet (choquet@ibpc.fr).

^{IV} Online version contains Web-only data.

www.plantcell.org/cgi/doi/10.1105/tpc.110.078170

impair respiratory growth in *S. cerevisiae* (reviewed in Ackerman and Tzagoloff, 2005; Fontanesi et al., 2008). Only a few such factors have been identified in mammals so far, but deficiency in the LRPPRC protein involved in the stabilization and translation of *coxI* and *coxIII* mRNAs is associated with severe diseases in human (Xu et al., 2004). Whether M and T factors are merely constitutively required for (i.e., control) mitochondrial or chloroplast gene expression or have true regulatory functions (i.e., regulate) is still a matter of debate. In *Chlamydomonas*, variations in the abundance of M and T factors with physiological conditions deeply impact the expression of their target gene (Raynaud et al., 2007). Likewise, in *S. cerevisiae*, the abundance of Pet111p is limiting in the expression level of *COXII* (Green-Willms et al., 2001), while that of Pet494p, governing the translation of *COXIII*, is modulated depending on the carbon source and oxygen availability (Steele et al., 1996).

In spite of their physiological importance, relatively little is known regarding the mode of action of these factors. Most of them belong to high molecular weight complexes, some of which contain an RNA moiety as well (Boudreau et al., 2000; Vaistij et al., 2000b; Auchincloss et al., 2002; Dauvillée et al., 2003; Perron et al., 2004). For instance, NAC2 and RBP40 belong to a single high molecular mass complex that also contains the *psbD* 5' untranslated region (UTR) (Schwarz et al., 2007).

Most T factors have been shown genetically to target the 5' UTR of the transcripts whose translation they assist, suggesting that they are required for the initiation of translation rather than for its elongation. Accordingly, RBP40, required for the synthesis of the D2 protein, may transiently interact with ribosomes (Schwarz et al., 2007) but is not found in polysomal fractions (Boudreau et al., 2000). However, the molecular events leading to translation initiation remain poorly understood. Some T factors may act by unmasking the initiation codon of their target mRNA, sequestered into a secondary structure (Stampacchia et al., 1997; Klinkert et al., 2006; Schwarz et al., 2007). Alternatively, T factors may recruit the translation machinery, but their affinity for components of this machinery remains to be documented in most cases (however, see McMullin et al., 1990; Haffter et al., 1991; Haffter and Fox, 1992).

According to an emerging consensus, M factors bind to the 5' or 3' termini of their target transcripts and stabilize them by acting as a barrier against exonucleases (Drager et al., 1998; Vaistij et al., 2000a; Loiselay et al., 2008; Hattori and Sugita, 2009; Pfalz et al., 2009). Whether, in addition, M factors participate in the translation of their target mRNA is still a matter of debate. In several instances, organelle transcripts in *Chlamydomonas* and *Saccharomyces*, even though engineered to accumulate in the absence of their stabilization factor, depend on the latter to be efficiently translated (Drager et al., 1998; Nickelsen et al., 1999; Vaistij et al., 2000a; Islas-Osuna et al., 2002).

To gain deeper insights into the function of M and T factors, we studied how MCA1 and TCA1 participate in the expression of the *petA* mRNA. We previously provided genetic evidence that these proteins target neighboring but distinct sequences in the very 5' end of *petA* 5'UTR, where they display partially overlapping functions in stabilization and translation of the *petA* mRNA (Loiselay et al., 2008): the MCA1-dependent accumulation of *petA* mRNA is reduced in the absence of TCA1, whereas

a modified *petA* transcript whose stability does not require the presence of MCA1 shows decreased TCA1-dependent rates of translation in the absence of MCA1 (Loiselay et al., 2008). Thus, MCA1 and TCA1, together with the *petA* transcript, should be regarded as the *petA* gene expression system. Here, we used biochemical and gene transformation approaches to provide the molecular basis for the interactions between the three components of the *petA* gene expression system, MCA1/TCA1/*petA* mRNA. In particular, we provide new evidence for a critical role of MCA1 in the regulation of *petA* mRNA translation, which allows us to relate the regulatory function of this M factor to the CES process for cytochrome *f* synthesis.

RESULTS

MCA1 and TCA1 Are Soluble Proteins

In mitochondria of *S. cerevisiae*, most *trans*-acting factors are associated with the inner membrane (Green-Willms et al., 2001; Naithani et al., 2003; Krause et al., 2004). In the green lineage as well, some chloroplast-targeted factors are membrane bound (Perron et al., 1999; Zerges et al., 2002; Balczun et al., 2005; Merendino et al., 2006). Since MCA1 and TCA1 are required for the synthesis of cytochrome *f*, an integral membrane protein, we first determined whether they behaved as soluble or membrane-bound proteins. To perform these studies, we used strains expressing tagged versions of MCA1 and TCA1, hereafter referred to as *mH* and *tF* that allow the immunological detection of these two factors (with apparent molecular masses of ~115 and ~110 kD, respectively) by antibodies directed against the HA or Flag epitopes. These strains (described in Supplemental Figure 1 online and in Raynaud et al., 2007) were obtained by complementation of *mca1* and *tca1* mutants, with HA- and Flag-tagged versions of *MCA1* and *TCA1*, respectively. As detailed in Methods, in the following, strains are named by their genotype. *m* (*t*) denotes mutated *MCA1* (*TCA1*) loci, whereas H (*F*) indicates that the *mca1* (*tca1*) mutations had been complemented by the HA-tagged version of *MCA1* (the Flag-tagged version of *TCA1*).

French press lysates of strains *mH* and *tF* were layered on top of a 1.5 M sucrose cushion (Figure 1). After ultracentrifugation, MCA1 and TCA1 were found in the supernatant *S_n*, as was the stromal chaperone GrpE (Schroda et al., 2001), while integral membrane proteins, like cytochrome *f*, were recovered mainly in the layer at the interface between the supernatant and the sucrose cushion (*M_b* in Figure 1). Thus, MCA1 and TCA1 behaved as soluble proteins.

Potential Interactions and Functional Domains of MCA1 and TCA1

As detailed in the introduction, MCA1 and TCA1 might synergistically bind to the *petA* 5'UTR (Loiselay et al., 2008). We tested their ability to interact physically by two-hybrid experiments in the yeast *S. cerevisiae*.

We cloned the whole coding sequences of MCA1 and TCA1 into GAL4-derived vectors, well suited for studying interactions between soluble proteins. In these experiments, interaction

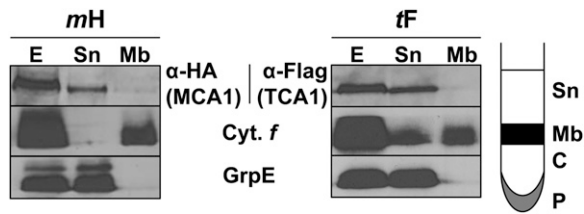


Figure 1. MCA1 and TCA1 Are Soluble Proteins.

Cell extracts (E) from *tF* and *mH* strains, overlaid on a 1.5 M sucrose cushion, were separated by ultracentrifugation into the fractions schematically depicted in the right panel. Sn, supernatant; Mb, membrane; C, cushion; P, pellet. Equal volumes of each fraction were immunoreacted with anti-HA or anti-Flag antibodies. In addition, GrpE and cytochrome *f* were used as markers of soluble and membrane fractions, respectively. In the *tF* (TCA1) panel, fraction Sn was slightly contaminated by membranes, which explains the presence of cytochrome *f* (Cyt. *f*). Fractions C and P are not shown, as they were devoid of significant amounts of MCA1, TCA1, GrpE, or cytochrome *f*.

between the tested proteins, respectively fused to the GAL4 activating domain (AD) and binding domain (BD), reconstitutes the GAL4 transcription factor that restores prototrophy for His and adenine (Figure 2). Strength of the interaction can be estimated by plating cells on media of increasing stringency (i.e., lacking His and supplemented with 3-amino-triazole [3-AT] or lacking both His and adenine). We observed that MCA1 interacts with itself as well as with TCA1 (Figure 2A). MCA1 homomeric interaction is consistent with our previous observation of a quadratic dependency of *petA* mRNA levels on MCA1 abundance in vivo (see Figure 3B in Raynaud et al., 2007). However, the BD-TCA1 fusion alone allowed growth of transformed yeast on the less stringent selective medium, which prevented us, in this first set of experiments, to study interaction of TCA1 with itself.

To characterize further the protein domains responsible for the interactions observed in Figure 2A, we repeated two-hybrid experiments with various truncated versions of TCA1 and MCA1. Indeed, protein interactions are sometimes better identified in the two-hybrid system with cDNAs expressing truncated proteins than with full-length cDNAs. The latter are often poorly expressed in *S. cerevisiae*, especially when they originate from organisms that display a widely different codon usage, such as *C. reinhardtii* (Fromont-Racine et al., 1997). We thus generated an N-terminal truncated version of TCA1, lacking the first 391 residues, hereafter referred to as CTCA1, which is still able to complement a *tca1*-null mutation (see Supplemental Figure 2 online). When fused to Gal4 BD and transformed into yeast, CTCA1 allowed growth on His-depleted but not on the more stringent medium lacking both His and adenine. By contrast, yeast cotransformed with both AD-CTCA1 and BD-CTCA1 constructs grew on this stringent medium (Figure 2B). Thus, TCA1 interacts with itself through its C-terminal domain, at least in *S. cerevisiae*. We failed to observe an interaction between the C-terminal domain of TCA1 and MCA1 (Figure 2B), suggesting that the N-terminal domain of TCA1 is required for the interaction with MCA1 that we observed in Figure 2A. Indeed, a C-terminal truncated version of TCA1, NTCA1, that retained only the first

391 residues fused to the GAL4-AD interacts with MCA1 (Figure 2B).

We similarly assessed the domains of MCA1 required for interactions with itself or with TCA1. We generated a C-terminal truncated version of MCA1, NMCA1, that lacks the last 290 residues (the last five Pentatricopeptide Repeats [PPR] and the

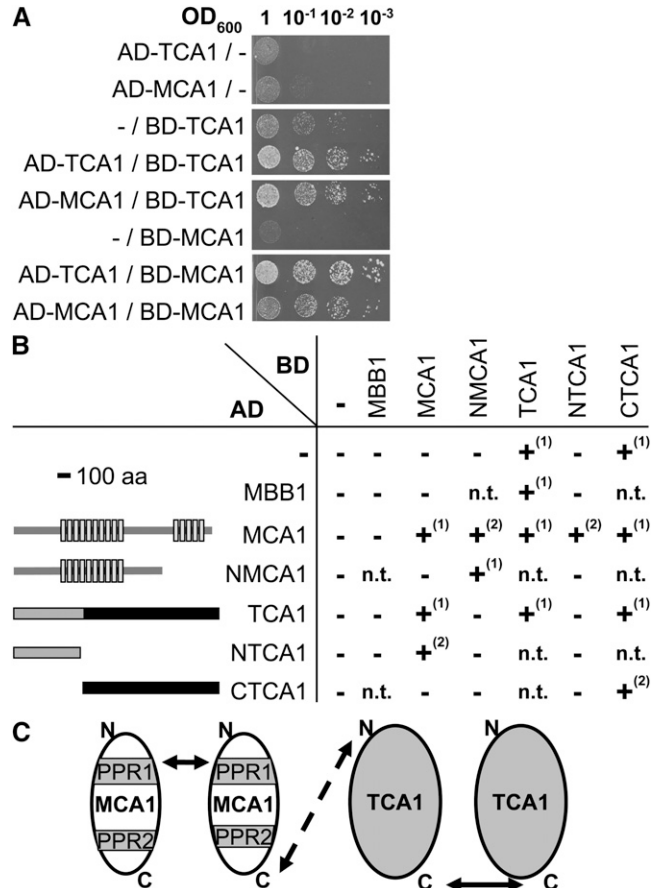


Figure 2. Interactions between MCA1 and TCA1 Probed by Two-Hybrid Experiments in Yeast.

(A) Interactions between full-length MCA1 and TCA1 proteins. Interactions were assessed between the proteins indicated at the left of the figure, fused either to the AD or to the BD of the *Gal4* transcription factor, by spotting serial dilutions of cotransformed yeast cells on selective medium (SD lacking Leu, Trp, and His but supplemented with 5 mM 3-AT).

(B) Interactions observed between the truncated versions of MCA1 and TCA1 schematically depicted at the left of the figure. Light-gray boxes depict the PPR repeats in the MCA1 protein, while the thick black bar indicates the shortest region of TCA1 still able to complement *tca1* mutations. Growth of transformed yeast was tested as above on different selective media: -, +⁽¹⁾, and +⁽²⁾ indicate the absence of growth on any selective media, growth on medium lacking His and supplemented with 3-AT, and growth on a more stringent medium lacking His and adenine. n.t., not tested; aa, amino acids.

(C) Schematic representation of MCA1/TCA1 interactions. PPR1 and 2 represent the two blocks of PPR repeats within MCA1. The dashed arrow points to an interaction suggested, but not fully demonstrated by our experiments, between the corresponding domains.

C-terminal tail). As shown in Figure 2B, NMCA1 still interacted with itself but had lost its ability to bind TCA1, suggesting that the C-terminal moiety of MCA1 is required for TCA1 recognition. Surprisingly, we observed an interaction between the AD-MCA1 and the BD-NMCA1 fusion proteins but not between AD-NMCA1 and BD-MCA1, which may originate from an altered folding of these fusion proteins that may prevent their interaction. The interactions developed by the various versions of MCA1 and TCA1 in the experiments shown in Figure 2 were specific for these two factors: we failed to detect any interaction of either MCA1 or TCA1 with MBB1, another nucleus-encoded factor specifically required for *psbB* mRNA stability in the chloroplast of *C. reinhardtii*.

Figure 2C schematically depicts the interactions between TCA1 and MCA1 identified by two-hybrid experiments in yeast. Homomeric interactions rely on protein domains distinct from those involved in hetero-interactions: the C-terminal moiety of MCA1 might interact with the N-terminal domain of TCA1, whereas these proteins interact with themselves through their N-terminal and C-terminal moieties, respectively. Together, these experiments suggested that MCA1 and TCA1 might associate in vivo in high molecular mass complexes.

MCA1 and TCA1 Form Oligomeric Complexes in the Presence and Absence of *petA* mRNA

Since two-hybrid experiments point to interactions between MCA1 and TCA1 in yeast cells, which are devoid of *petA* mRNA, we used coimmunoprecipitation (CoIP) to assess their ability to interact in vivo in the absence of the *petA* transcript.

To this end, we constructed a double mutant strain, *mt*, lacking both MCA1 and TCA1 (Table 1). We then recovered a strain expressing MCA1-HA in the absence of TCA1, *mHt*, among the progeny of a cross between strain *mH* and the *mt* double mutant. We similarly recovered the *mtF* strain, expressing TCA1-FI in the absence of MCA1. The *petA* gene was then deleted in these two strains by biolistic transformation to generate strains *mHt* { $\Delta petA$ } and *mtF* { $\Delta petA$ } that express MCA1-HA or TCA1-FI, respectively, in the absence of both interacting partners (Table 2). Soluble extracts from these strains were mixed before performing CoIPs with anti-HA or anti-Flag antibodies coupled to sepharose beads. The precipitates were analyzed by protein gel blots probed with anti-HA, anti-Flag, or anti-NAC2 antibodies (Figure 3A). TCA1, but not NAC2, was detected in the pellet after anti-HA precipitation, as was MCA1 after anti-Flag precipitation.

Table 1. *C. reinhardtii* Strains Generated by Crosses

| Mating Type– Parent | Mating Type+ Parent | Resulting Strain |
|---------------------|---------------------|---|
| <i>tca1-8</i> | <i>mca1-6</i> | <i>mt</i> |
| <i>mt</i> | <i>mH</i> | <i>mHt</i> |
| <i>mt</i> | <i>tF</i> | <i>mtF</i> |
| <i>mH</i> | { <i>ccsA-B6</i> } | <i>mH</i> { <i>ccsA-B6</i> } ^a |

^aDue to the uniparental inheritance of the chloroplast genome from the *mt+* parent strain, each member of the resulting tetrads carried the chloroplast mutation *ccsA-B6*, while the two nuclear loci *mca1-8* and MCA1-HA showed independent Mendelian segregation.

Thus, the two proteins have a high affinity for each other, since they specifically interact in the absence of the *petA* transcript after mixing cell lysates in which preexisting interactions were prevented.

In presence of the *petA* mRNA, interactions between MCA1 and TCA1 were further confirmed by the same CoIP approach using soluble extracts from a double-complemented *mHtF* strain that expresses both MCA1-HA and TCA1-FI, using strains *mH* and *tF* as controls (Figure 3B). Antibodies directed against MCA1-HA pulled down TCA1 using extracts from strain *mHtF* but not from the control strain *tF*. Similarly, MCA1 was coimmunoprecipitated by antibodies directed against TCA1-FI in soluble extracts from strain *mHtF* but not from the control strain *mH*. Thus, MCA1 and TCA1 do interact in vivo when the *petA* mRNA is present.

MCA1 and TCA1 Belong in Vivo to Large Complexes That Also Contain *petA* mRNA

We then used size exclusion chromatography to characterize the protein complexes formed upon association of TCA1 with MCA1. Supernatants recovered after centrifugation of French press lysates from *tF* and *mH* cells were fractionated on a Sephacryl S500 column (GE Healthcare), optimal for separating protein complexes in the 100 to 10,000 kD range. As shown in Figure 4 (samples 5 and 12), MCA1 and TCA1 belong to high molecular mass complexes peaking in fractions 10 and 11 with an apparent molecular mass of ~600 kD, a size similar to that of the complexes containing NAC2, used here as a control and internal standard (sample 6; Boudreau et al., 2000).

The presence of RNAs, in particular *petA* mRNA, in these high molecular mass complexes was investigated by two different approaches. First, we RNase treated the soluble extracts from *mH* and *tF* strains, prior to size exclusion chromatography (samples 3 and 11). We also analyzed soluble extracts from strains *mH* { $\Delta petA$ } and *tF* { $\Delta petA$ }, lacking the *petA* gene (samples 2 and 10). In all instances, we observed a broadening in the distribution of MCA1 and TCA1, with a shift toward heavier fractions peaking around 1200 kD. By contrast, the distribution of NAC2 (sample 7) shifted toward fractions of lower molecular mass upon RNase treatment, as previously reported (Boudreau et al., 2000). Thus, the presence of *petA* mRNA is responsible for the typical distribution of complexes containing MCA1 and TCA1 peaking at 600 kD that we observed in strains *mH* and *tF*.

MCA1 and TCA1 probably shifted toward fractions of higher molecular mass in the absence of the *petA* mRNA because they develop homo- and hetero-interactions as we observed by CoIP and two-hybrid experiments in yeast (Figures 2 and 3B). To distinguish homo-oligomers of similar apparent molecular mass containing either MCA1 only or TCA1 only from hetero-oligomers comprising both proteins, we analyzed the distribution of MCA1 in the absence of both TCA1 and *petA* or of TCA1 in the absence of both MCA1 and *petA* (strains *mHt* { $\Delta petA$ } and *mtF* { $\Delta petA$ }, respectively; samples 1 and 8 in Figure 4). In these strains, MCA1 and TCA1 were no longer found in broadly distributed protein complexes centered around 1200 kD but within lighter protein complexes of ~500 kD. Similar protein complexes were found in strains *mHt* and *mtF* that express MCA1-HA in the absence of TCA1 or TCA1-FI in the absence of MCA1 and, consequently,

Table 2. *C. reinhardtii* Strains Generated by Transformation

| Recipient Strain | Transforming Plasmid | Transformed Strains |
|---|--|--|
| Nuclear transformation ^a | | |
| <i>mca1-6</i> | plgMCA1-HA [1] ^b | <i>mH</i> |
| <i>mtF</i> | plgMCA1-HA [1] ^b | <i>mHtF</i> |
| <i>tca1-8</i> | pshTCA1-FI [1] ^c | CTCA1 |
| Chloroplast transformation ^d | | |
| <i>mH</i> | p Δ <i>petA</i> [2] | <i>mH</i> { Δ <i>petA</i> } ^e |
| <i>mH</i> | pWF _{StoP} K [this study] | <i>mH</i> { <i>petA</i> _S } ^e |
| <i>mH</i> | p5' <i>dAf</i> K [this study] | <i>mH</i> {5' <i>dAf</i> } ^f |
| <i>mH</i> | p <i>f</i> ₂₈₃ St [3] | <i>mH</i> { <i>f</i> ₂₈₃ } ^{e,g} |
| <i>mH</i> | p <i>f</i> ₃₁₂ St [4] | <i>mH</i> { <i>f</i> ₃₁₂ St} ^g |
| <i>mH</i> | p <i>f</i> ₃₁₀ St [4] | <i>mH</i> { <i>f</i> ₃₁₀ St} ^g |
| <i>mH</i> | p <i>f</i> ₃₀₇ St [4] | <i>mH</i> { <i>f</i> ₃₀₇ St} ^g |
| <i>mH</i> | p <i>f</i> ₃₀₄ M [4] | <i>mH</i> { <i>f</i> ₃₀₄ M} ^h |
| <i>mH</i> | p <i>f</i> ₃₀₇ S [4] | <i>mH</i> { <i>f</i> ₃₀₇ S} ^h |
| <i>mH</i> | p <i>f</i> Δ K [4] | <i>mH</i> { <i>f</i> Δ K} ^h |
| <i>mH</i> | p5' <i>dAf</i> ₃₀₇ S [this study] | <i>mH</i> {5' <i>dAf</i> ₃₀₇ S} ^{f,h} |
| <i>mH</i> | p Δ <i>petD</i> [2] | <i>mH</i> { Δ <i>petD</i> } ^e |
| <i>mHt</i> | p Δ <i>petA</i> [2] | <i>mHt</i> { Δ <i>petA</i> } ^f |
| <i>mHt</i> | p5' <i>dAf</i> K [this study] | <i>mHt</i> {5' <i>dAf</i> } ^{f,i} |
| <i>mHt</i> | p5' <i>dAf</i> ₃₀₇ S [this study] | <i>mHt</i> {5' <i>dAf</i> ₃₀₇ S} ^{h,i} |
| <i>tF</i> | p Δ <i>petA</i> [2] | <i>tF</i> { Δ <i>petA</i> } ^e |
| <i>mtF</i> | p Δ <i>petA</i> [2] | <i>mtF</i> { Δ <i>petA</i> } ^f |

References are as follows: 1 (Raynaud et al., 2007), 2 (Kuras and Wollman, 1994), 3 (Kuras et al., 1995a); 4 (Choquet et al., 2003), and 5 (Loisel et al., 2008).

^aAll recipient strains were nonphotosynthetic, and transformants were selected for photoautotrophy on minimum medium (Harris, 1989) under high light (200 μ E·m⁻²·s⁻¹).

^bPlasmid DNA was linearized with *Xba*I that cuts upstream of the MCA1 initiation codon before transformation.

^cPlasmid was cut with *Xba*I and *Sfi*I, and the 5461-bp fragment that encodes the C-terminal domain of TCA1 was used for transformation after gel purification.

^dAll recipient strains were spectinomycin sensitive. Transformed strains were selected for resistance to spectinomycin (100 μ g·mL⁻¹) under low light (5 μ E·m⁻²·s⁻¹) and subcloned in darkness until they reached homoplasmy, unless otherwise indicated.

^eHomoplasmy was deduced from the loss of photoautotrophic growth capacity.

^fHomoplasmy was assessed by RNA gel blot experiments.

^gHomoplasmy was assessed by protein immunoblot analysis for the expression of truncated versions of cytochrome *f*.

^hThe presence of the *f*₃₀₇S substitution was screened by restriction fragment length polymorphism analysis of PCR products amplified with primers Test_*petA*_For and Test_*petA*_Rev, as described by Choquet et al. (2003 [see Supplemental Table A]).

ⁱStrains were subcloned under dim light (25 μ E·m⁻²·s⁻¹) as recipient strains were nonphotosynthetic mutants, whereas the transformed strains regained photoautotrophic growth capability.

show little or no accumulation of *petA* mRNA (samples 4 and 9). Thus, the heavy complexes in the 1200 kD range likely correspond to hetero-oligomers of MCA1 and TCA1 that formed in the absence of the *petA* mRNA.

In summary, the three components of the *petA* gene expression system (MCA1, TCA1, and the *petA* transcript), when present all together, are engaged in a ternary complex of ~600 kD, which may accommodate dimers of each protein and one or

two copies of the *petA* 5'UTR. Note that in these experiments, no special care was taken to preserve the integrity of the RNA moiety: the *petA* mRNA was likely trimmed to the transcript portions protected from degradation by their interaction with nucleus-encoded factors. Thus, RNA fragments retained in the ternary complex in these experiments are most probably restricted to the *petA* 5'UTR and should account for <100 kD.

In the absence of *petA* transcripts, MCA1 and TCA1 are likely to form large hetero-oligomeric complexes ranging from several MD to ~100 kD, centered around 1200 kD. This broad distribution suggests variable states of aggregation of these factors, which may also associate with additional proteins. We note that our size exclusion chromatography experiments poorly resolve changes in the distribution of MCA1 and TCA1 in the 500- to 600-kD range between strains *mH*, *tF*, *mHt*, and *mtF*. These distributions nevertheless corresponded to widely different protein populations since we obtained experimental evidence for a ternary complex in the former two strains as opposed to homo-oligomers, possibly tetramers, in the latter two strains.

Mutual Stabilization of MCA1 and TCA1

We then studied the accumulation of MCA1 and TCA1 in the absence of their partners from the ternary complex. As shown in Figures 3A and 4 (samples 1 and 4), MCA1 still accumulates to detectable levels in the absence of TCA1 and/or *petA* mRNA. Similarly, TCA1 shows notable accumulation in the absence of MCA1 and/or *petA* mRNA (Figures 3A and 4, samples 8 and 9). Because MCA1 and TCA1 belong to distinct complexes when expressed alone or together with *petA* mRNA, their proteolytic

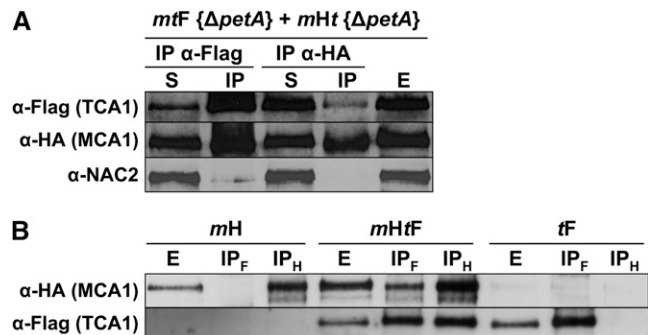


Figure 3. Interactions among MCA1, TCA1, and *petA* mRNA Probed by CoIP.

(A) MCA1 and TCA1 interact in the absence of *petA* mRNA. Equal volumes of *mtF* { Δ *petA*} and *mHt* { Δ *petA*} cultures were mixed and broken with a French press. The soluble extract recovered after centrifugation (E) was immunoprecipitated with anti-HA or anti-Flag antibodies, as indicated. The presence of MCA1/TCA1 in supernatant (S) and immunoprecipitated (IP) fractions was then assessed using the same antibodies, as indicated at the left of the figure. The antibody against the NAC2 protein provided a specificity control.

(B) Interactions between MCA1 and TCA1 in the presence of the *petA* mRNA. Soluble extracts (E) from strains *mH*, *mHtF*, and *tF* and immunoprecipitates recovered after incubation of the extracts with either anti-HA (IP_H) or anti-Flag (IP_F) antibodies were analyzed as above for the presence of MCA1 and TCA1.

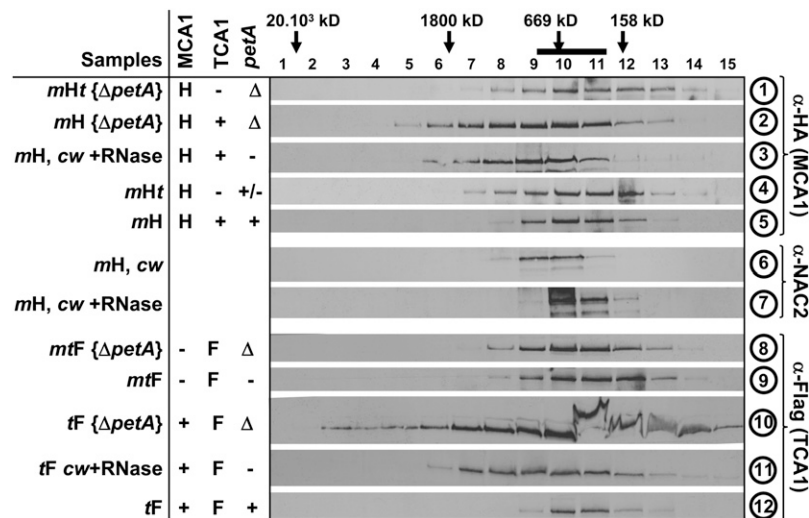


Figure 4. Interactions between MCA1, TCA1, and the *petA* mRNA Probed by Size Exclusion Chromatography.

Soluble or stromal (prepared from *cw* strains lacking cell wall) extracts from strains listed at the left of the figure were fractionated on Sephacryl S500 column and analyzed with the antibodies indicated at the right of the figure. Molecular masses of the complexes found in each fraction were estimated by comparison with standards of the HMW gel filtration calibration kit (GE Healthcare) or with the position of ribulose-1,5-bisphosphate carboxylase/oxygenase (indicated by the thick black bar at the top of the figure). The middle table recapitulates the status of each partner of the *petA* gene expression system: MCA1 (Δ /TCA1) is absent (-) or expressed from the wild-type (+) or tagged (H/F) gene, while the *petA* mRNA is either absent in deletion strains (Δ) or in the absence of MCA1 (-), present in reduced amounts in the absence of TCA1 (+/-), or accumulated to wild-type levels (+).

susceptibilities and, hence, their accumulation levels may vary depending on these interactions.

We first compared the extent of accumulation of TCA1 in the presence or absence of MCA1. As shown in Figure 5A, TCA1 accumulation was identical in strains *tF* and *mtF*, this latter strain also lacking *petA* mRNA, destabilized in the absence of MCA1. To sort out the consequences of the absence of MCA1 versus defective cytochrome *f* expression, we analyzed the strain *tF* { Δ *petA*} and observed a 3-fold increased accumulation of TCA1 when compared with strains *tF* and *mtF* (Figure 5B). Both strains *mtF* and *tF* { Δ *petA*} lack *petA* mRNA, but only strain *tF* { Δ *petA*} expresses MCA1. We conclude that, in absence of *petA* mRNA, the presence of MCA1 stabilizes TCA1, most probably by allowing the formation of the stable ~1200-kD oligomers that we detected by size exclusion chromatography.

Strikingly, the steady state level of MCA1, as detected in strain *mH*, increased 10-fold in the absence of *petA* mRNA (strain *mH* { Δ *petA*}) and 3-fold in the absence of TCA1, irrespective of the presence of *petA* mRNA (strains *mHt* and *mHt* { Δ *petA*}; Figure 5C). The much higher accumulation of MCA1 in strain *mH* { Δ *petA*} than in strain *mHt* { Δ *petA*} or *mHt*, the three of which are defective for cytochrome *f* expression, suggested that, in the absence of cytochrome *f*, MCA1 is stabilized by TCA1 most probably again within the ~1200-kD high molecular mass complexes. However, this stabilizing effect of TCA1 was not observed when comparing strains *mH* and *mHt*, since the level of MCA1 was 3 times higher in the latter, which lacks TCA1. If one takes into account that cytochrome *f* is expressed in strain *mH*, but not in strain *mHt*, then these contrasting observations can be reconciled by assuming that the steady state level of accumulation of MCA1 results from two opposite effects: (1) a

contribution of TCA1 to the stability of MCA1 and (2) a degradation of MCA1 upon cytochrome *f* expression, which also depends on TCA1. In strain *mH*, although the two contributions are at work, the expression of cytochrome *f* would lead to an extensive proteolytic disposal of MCA1.

Cytochrome *f* Expression Shortens the Half-Life of MCA1

To investigate further the possible role of cytochrome *f* expression in MCA1 degradation, we transformed the chloroplast genome of strain *mH* with a modified *petA* gene that cannot be translated because its initiation codon has been replaced by a Stop codon. In the resulting *mH* {*petA*_{SS}} strain, despite the accumulation of the untranslatable *petA* mRNA, MCA1 is 10 times more abundant than in a wild-type genetic context, reaching the same high level as in the absence of *petA* mRNA (Figure 6A). To confirm that MCA1 is degraded upon cytochrome *f* expression, we compared the decay of MCA1 in various regimes for *petA* mRNA translation by immunochase experiments in the presence of cycloheximide that prevents cytosolic translation and, therefore, de novo synthesis of MCA1. As previously reported (Raynaud et al., 2007), MCA1 expressed in a wild-type context is short lived, with a half-life in the hour range (Figure 6B, panel *mH*). By marked contrast, MCA1 remained stable over 6 h of chase in the absence of cytochrome *f* expression in strains *mH* {*petA*_{SS}} or *mH* { Δ *petA*}. Moreover, when the translation-competent *mH* strain was incubated with cycloheximide and lincomycin to prevent both cytosolic and chloroplast translations (bottom of Figure 6B), the half-life of MCA1 increased markedly, when compared with the control culture treated with cycloheximide alone. Thus, cytochrome *f* expression targets MCA1 for degradation.

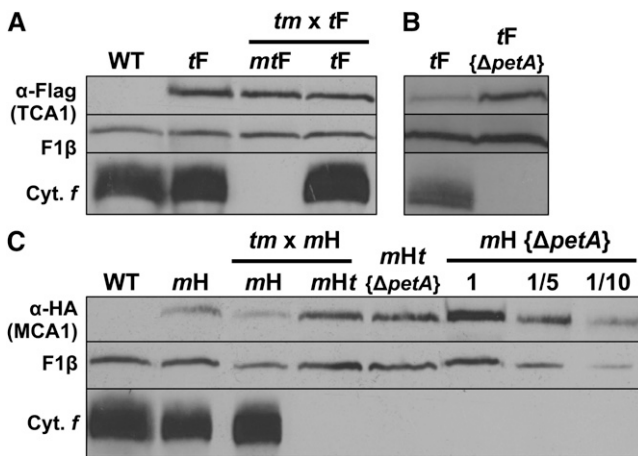


Figure 5. The Accumulation of MCA1 or TCA1 Depends on the Presence of Their Partners from the *petA* Gene Expression System.

(A) and (B) Immunoblots showing accumulation of TCA1-FI in an otherwise wild-type genetic context (strain *tF*), in progeny expressing TCA1-FI of one representative tetraploid recovered after crossing *mt* and *tF* strains (A), or in the absence of *petA* mRNA (strain *tF* $\{\Delta petA\}$; [B]). The *mtF* progeny lacking MCA1 also lacks cytochrome *f*.

(C) Accumulation of MCA1-HA in strains with an otherwise wild-type genetic context (*mH*), lacking *petA* (*mH* $\{\Delta petA\}$), both *petA* and TCA1 (*mHt* $\{\Delta petA\}$), and in the progeny expressing MCA1-HA of one representative tetraploid tetrad from the cross *mt* \times *mH*. The *mHt* progeny that inherited the mutant *tca1* allele from the *mt* parent lacks cytochrome *f*. A dilution series of the *mH* $\{\Delta petA\}$ sample is shown for the ease of quantification.

For both panels, expression of cytochrome *f* (cyt. *f*) and of the β -subunit of the mitochondrial ATP synthase complex (F1 β ; loading control) is also shown. The wild-type strain (WT) that does not express MCA1-HA or TCA1-FI is shown as a control.

MCA1 Degradation Does Not Result from Its Interaction with the *petA* 5'UTR

To identify the pathway that leads to MCA1 degradation upon cytochrome *f* expression, we first investigated whether it required the action of MCA1 on its 5'UTR target on the *petA* mRNA. We replaced by biolistic transformation the endogenous *petA* gene in the *mH* strain by a chimeric version 5'*dAf* in which the *petA* coding sequence is fused to the 5'UTR of the unrelated *atpA* gene (Choquet et al., 1998; Drapier et al., 2007). Since the targets of MCA1 and TCA1 lie within the *petA* 5'UTR, these transacting factors are no longer involved in the expression of the 5'*dAf* chimera (Wostrikoff et al., 2001; Loiselay et al., 2008). The resulting strain *mH* {5'*dAf*} was analyzed for MCA1 content and half-life. When compared with the *mH* strain, it displayed the same low level (Figure 6A) of short-lived (Figure 6B) MCA1. Thus, MCA1 is still degraded in this strain, although it is no longer involved in cytochrome *f* synthesis.

Then, we preserved translation of the *petA* gene but introduced by transformation a premature termination codon in the *petA* coding sequence. This led to the expression of a soluble variant of cytochrome *f*, *f*_{sol}, that lacks the stromal-exposed C-terminal tail and the transmembrane helix anchoring the

luminal domain of cytochrome *f* into the membrane (Kuras et al., 1995a). In the *mH* {*f*_{sol}} strain, the accumulation of MCA1 was much increased with respect to the *mH* recipient strain and became similar to that detected in the *mH* $\{\Delta petA\}$ strain (Figure 6A), as a result of the increased life-time of MCA1 (Figure 6B). Thus, the degradation of MCA1 is not triggered by translation initiation but rather by the expression of the C-terminal domain of cytochrome *f*.

MCA1 Is Degraded upon Interaction with Specific Residues in the C-Terminal Domain of Cytochrome *f*

To get further insight into the residues of cytochrome *f* involved in the degradation of MCA1, we took advantage of previously constructed versions of cytochrome *f* lacking the last 6, 8, or 11 amino acids of the stromal tail (Choquet et al., 2003; Figure 7A). These mutated *petA* genes were introduced by biolistic transformation into the chloroplast genome of the *mH* recipient strain to yield strains *mH* {*f*_{312St}}, *mH* {*f*_{310St}}, and *mH* {*f*_{307St}},

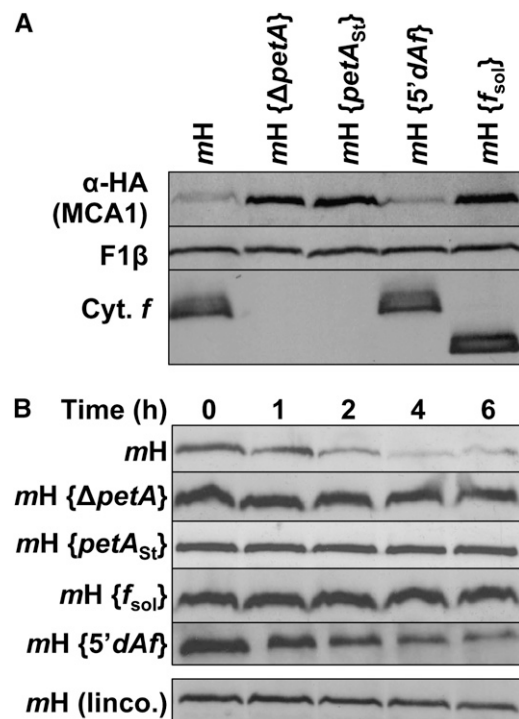


Figure 6. Half-Life and Accumulation of MCA1 Are Governed by the Expression of Full-Length Cytochrome *f*.

(A) Accumulation of MCA1-HA in an otherwise wild-type strain (*mH*), in strains carrying a *petA* gene deletion (*mH* $\{\Delta petA\}$) or expressing a modified *petA* gene that (1) cannot be translated (*mH* {*petA*_{St}}), (2) is expressed under the control of the *atpA* 5'UTR (*mH* {5'*dAf*}), or (3) encodes a truncated soluble cytochrome *f* (*mH* {*f*_{sol}}). Accumulation of cytochrome *f* (Cyt. *f*) in the various strains is shown, while the β -subunit of the mitochondrial ATP synthase complex (F1 β) provides a loading control.

(B) Half-life of MCA1 assessed in the same strains by immunochase at the various time points indicated after addition at *t* = 0 of cycloheximide alone or of cycloheximide plus lincomycin (linco.).

respectively. Whereas the shortest truncation $f_{312}\text{St}$ did not affect the accumulation of MCA1, which remained similar to that observed in the recipient mH strain, the intermediate truncation, $f_{310}\text{St}$, induced a twofold increase in MCA1 accumulation, and the largest truncation, $f_{307}\text{St}$, led to an ~ 10 -fold higher accumulation of MCA1 (Figure 7B), as observed in the $mH \{\Delta\text{petA}\}$ strain (Figure 6A).

Strikingly, the very same truncations led to a progressive loss of the CES control of cytochrome f synthesis, a process that couples the rate of cytochrome f synthesis to its assembly into the cytochrome b_6f complex. This regulatory process involves the 5'UTR of the petA mRNA (Choquet et al., 1998) and a repressor domain exposed by unassembled cytochrome f , made of a few specific amino acids from the C-terminal domain of the protein. These residues are shown in Figure 7A in black when their substitutions strongly affect the cytochrome f CES process or in gray when substitutions have a significant but more limited effect on this regulatory process (Choquet et al., 2003). Whether these specific residues are also involved in MCA1 degradation was investigated by biolistic transformation of strain mH with petA constructs harboring the corresponding point mutations

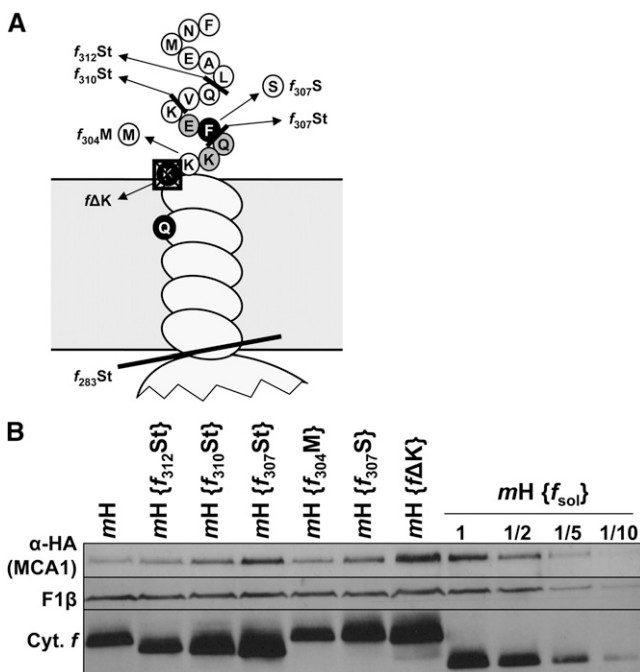


Figure 7. Disruption of the CES Repressor Domain Stabilizes MCA1.

(A) Schematic representation of the mutations introduced in the stromal-exposed C-terminal tail of cytochrome f in strain mH . Substitutions of the residues shaded in black abolish the cytochrome f CES process, whereas mutations of those shaded in gray attenuate this regulatory process (Choquet et al., 2003).

(B) Accumulation of MCA1-HA in strains with an otherwise wild-type background (strain mH) or carrying the mutations depicted in **(A)**. A dilution series of the strain $mH \{f_{\text{sol}}\}$ is shown for the ease of quantification. Note that strain $mH \{f\Delta K\}$ was slightly overloaded in this gel. Cyt., cytochrome.

within the sequence coding for cytochrome f . As shown on Figure 7B, substitution of Lys-304 by a Met, which does not impact the CES process (Choquet et al., 2003), did not alter the accumulation of MCA1 either (compare strain $mH \{f_{304}\text{M}\}$ with strain mH). By contrast, two mutations that compromise the assembly-dependent regulation of cytochrome f synthesis also increased the accumulation of MCA1: substitution of Phe-307 by a Ser led to a 3-fold increase in the accumulation of MCA1 (strain $mH \{f_{307}\text{S}\}$), whereas deletion of one of the three Lys residues just after the transmembrane helix (strain $mH \{f\Delta K\}$) resulted in the same 10-fold overaccumulation of MCA1 than in strain $mH \{\Delta\text{petA}\}$ (Figure 6A).

We thus conclude that the same C-terminal motif in the sequence of cytochrome f is involved in the CES process and in the degradation of MCA1.

Degradation of MCA1 Depends on the Level of Accumulation of the Unassembled CES Repressor Motif

To determine whether the level of accumulation of the unassembled CES repressor domain or its mere synthesis is responsible for the degradation of MCA1, we compared the level of accumulation of MCA1 under two experimental situations that lead to the most contrasting rates of cytochrome f translation due to extensive changes in the accumulation level of its CES repressor motif.

When holocytochrome f formation is prevented, either because the Cys ligands of the c-type heme are substituted or because mutations inactivate the CCS machinery required for covalent heme binding to apocytochrome f (Kuras et al., 1995b; Xie et al., 1998), the resulting apocytochrome f is rapidly degraded. Consequently, the CES repressor domain accumulates to $<0.5\%$ of its level in the wild type, which results in a 3-fold increase in the rate of cytochrome f translation (Kuras et al., 1995b; Choquet et al., 1998). By contrast, in the $mH \{\Delta\text{petD}\}$ strain lacking subunit IV, in which cytochrome f remains unassembled, the repressor domain is particularly long lived, and cytochrome f synthesis is 10 times repressed due to the CES process.

We therefore crossed the mH strain with the mutant strain $\{ccsA\text{-B6}\}$ defective for the CCS pathway because of a premature Stop codon in the chloroplast ccsA gene (Xie et al., 1998) and also deleted the petD gene in the same mH strain by chloroplast transformation. Accumulation of MCA1 was increased in strain $mH \{ccsA\text{-B6}\}$ (Figure 8A) but decreased 2 to 3 times in strain $mH \{\Delta\text{petD}\}$ (Figure 8B), with respect to that in the parental strain mH . Moreover, at variance to its behavior in the mH recipient strain, the half-life of MCA1 was not increased when chloroplast translation was inhibited by addition of lincomycin in strain $mH \{\Delta\text{petD}\}$ (Figure 8C). It appears that the preexisting and long-lived CES repressor domain keeps targeting MCA1 for degradation.

MCA1-Induced Variations in petA mRNA Abundance

Since the primary function of MCA1 is the stabilization of the petA mRNA, even if it also acts as a translational enhancer (Loiselay et al., 2008), the above-described changes in MCA1 abundance (Figures 7 and 8B) also should cause changes in the

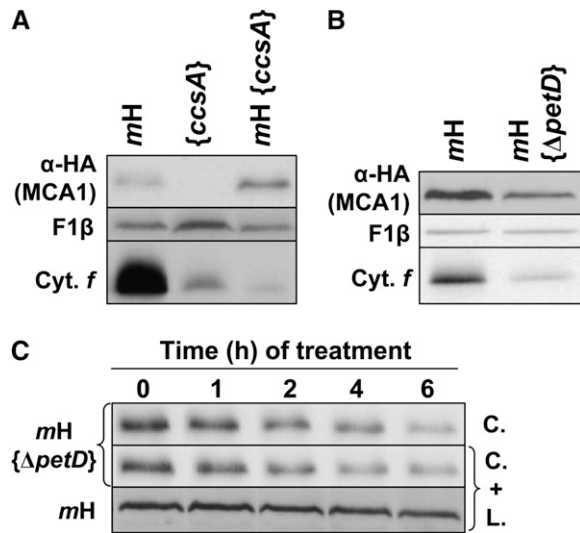


Figure 8. Accumulation and Half-Life of MCA1 Are Governed by the Accumulation of the CES Repressor Motif.

(A) Accumulation of MCA1-HA and cytochrome *f* (Cyt. *f*) in a double mutant *mH*, *{ccsA-B6}*, and in the parental strains *mH* and *{ccsA-B6}*.

(B) Accumulation of MCA1-HA and cytochrome *f* in strains *mH* and *mH {ΔpetD}*.

In both panels, the accumulation of the β-subunit of the mitochondrial ATP synthase complex (F1β) provides a loading control.

(C) Half-life of MCA1-HA assessed in strains *mH* and *mH {ΔpetD}* by immunochase experiments in the presence of cycloheximide (C.) or both cycloheximide and lincomycin (C.+L.).

accumulation of its target transcript. We thus analyzed by RNA gel blots the accumulation of *petA* transcripts in diagnostic strains from Figures 7 and 8B. We chose the *mH* strain as a reference, the *mH {ΔpetD}* as an archetype of a strain where the synthesis of cytochrome *f* is repressed because of the CES process, and the three deletion strains, *mH {f₃₁₂St}*, *mH {f₃₁₀St}*, and *mH {f₃₀₇St}* to assess the consequences of a progressive disruption of the CES repressor domain (Figure 9). We observed that the accumulation of the *petA* mRNA was reduced 2-fold in strain *mH {ΔpetD}* when compared with the reference strain *mH*, whereas it increased progressively as truncations extended into the repressor motif, reaching 250% of the wild-type level in strain *mH {f₃₀₇St}*. However, we note that in strain *mH {ΔpetD}*, the 2-fold reduction in *petA* transcript level cannot alone account for the 10-fold decreased rate of cytochrome *f* synthesis, as expected for a regulation operating mainly at the translational level. By contrast, in strain *mH {f₃₀₇St}*, the 2.5-fold increase in *petA* mRNA was comparable to the increase in cytochrome *f* synthesis rate, but we had previously shown that there is little correlation, in an otherwise wild-type genetic context, between the accumulation and the translation of the *petA* mRNA (Sturm et al., 1994).

Interaction between MCA1 and Unassembled Cytochrome *f* Does Not Require TCA1

The interaction between unassembled cytochrome *f* and MCA1 could be restricted to this factor alone, or it could involve a high

molecular mass complex that also contains TCA1. We addressed that point using the 5'*dAf* chimera, which allows the synthesis of cytochrome *f* in the absence of TCA1. We introduced in the *petA* coding sequence of this chimera the Phe-307 to Ser substitution that abolishes the CES regulation of endogenous cytochrome *f* expression and its interaction with MCA1, to yield the 5'*dAf*_{307S} chimera that was transformed into the chloroplast of strain *mH*. Compared with the low level of short-lived MCA1 in strain *mH* {5'*dAf*} (Figure 6), the immunoblot analysis of the transformed strains revealed a much higher accumulation of MCA1 in strain *mH* {5'*dAf*_{307S}} (Figure 10), confirming that MCA1 still interacts with the C-terminal domain of the 5'*atpA*-driven cytochrome *f*.

The same 5'*dAf* and 5'*dAf*_{307S} constructs were then transformed into strain *mHt*, lacking TCA1, and the resulting transformants were analyzed by immunoblots. We note that MCA1 was less abundant in strains *mHt* {5'*dAf*} and *mHt* {5'*dAf*_{307S}} than in strains *mH* {5'*dAf*} and *mH* {5'*dAf*_{307S}}, respectively, due to the above-described stabilization of MCA1 by TCA1. However, the accumulation of MCA1 was much higher when the CES repressor motif was mutated in strain *mHt* {5'*dAf*_{307S}} than when it was preserved in strain *mHt* {5'*dAf*} (Figure 10), demonstrating that MCA1 does not require TCA1 for its interaction with the CES repressor motif that regulates its rate of degradation.

DISCUSSION

MCA1 and TCA1 Participate with *petA* mRNA in the Formation of the *petA* Gene Expression System

Our previous studies of the nuclear control of cytochrome *f* expression led to the genetic characterization of two nucleus-encoded factors, MCA1 and TCA1, whose combined actions in *Chlamydomonas* chloroplasts allow accumulation of the *petA* mRNA in a translatable form (Loiselay et al., 2008). Here, we further characterized the resulting *petA* gene expression system by taking advantage of the availability of complemented strains expressing tagged versions of each protein. The transient molecular interactions that may develop during the formation of the

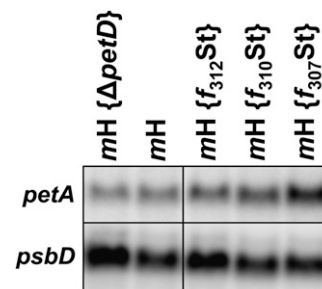


Figure 9. *petA* Transcript Accumulation in Representative Strains.

Accumulation of *petA* mRNA in representative strains analyzed in Figures 7B and 8B. A probe specific for the *psbD* transcript provides a loading control. Note the overloading of sample *mH {ΔpetD}* and to a lesser extent of sample *mH {f₃₁₂St}*.

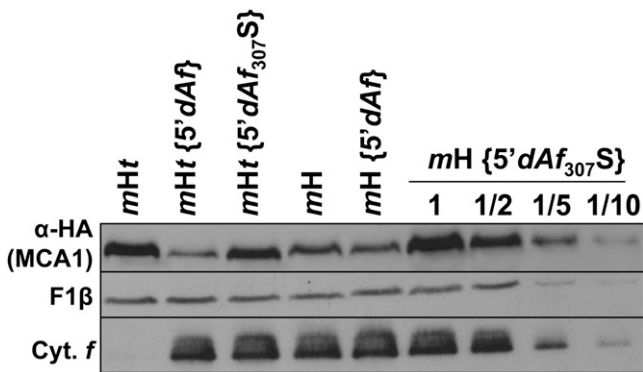


Figure 10. Destabilization of MCA1 by the Cytochrome *f* C Terminus Does Not Require the Presence of TCA1.

Accumulation of MCA1-HA, in an otherwise wild-type background (strain *mH*), in strains where *petA* coding sequence is expressed under the control of the *atpA* 5'UTR (strain *mH* {5'*dAf*}) and additionally carries a mutation preventing the CES process (strain *mH* {5'*dAf*_{307S}}). A dilution series is shown for strain *mH* {5'*dAf*_{307S}}. The same chloroplast genotypes were also compared in the *mHt* nuclear background (i.e., in the absence of TCA1). Accumulations of cytochrome *f* (Cyt. *f*) and subunit β of the mitochondrial ATP synthase (F1β, loading control) are also shown in the various strains.

petA gene expression system are described in the working model presented in Figure 11.

Our biochemical studies suggest that cytochrome *f* synthesis depends on a ternary complex (~600 kD) comprising MCA1 and TCA1 together with the *petA* transcript. Size exclusion chromatography experiments suggest that MCA1 interacts with the *petA* 5'UTR *in vivo* (Figure 4), even if it remains to be understood whether this interaction is direct or indirect. From its size of ~600 kD, this ternary complex may contain two copies of MCA1 and TCA1, as well as one or two copies of the *petA* mRNA. Indeed, MCA1 and TCA1 interact through the N-terminal moiety of TCA1 that recognizes MCA1, probably via its PPR-containing C-terminal domain. Since this interaction has been observed in *S. cerevisiae* by two-hybrid experiments, binding to *petA* mRNA is not a prerequisite for MCA1/TCA1 recognition; indeed, MCA1 and TCA1 can be coimmunoprecipitated in the absence of *petA* mRNA. These observations are consistent with the association of TCA1 and MCA1, after RNase treatment or in *petA* deletion strains, in heavy protein complexes that are probably heterogeneous in size, as shown by their broad distribution around 1200 kD. Moreover, the C-terminal region of TCA1, which does not interact with MCA1 in the yeast two-hybrid system, can still complement *tca1* null mutants (see Supplemental Figure 2 online). Thus, MCA1–TCA1 interactions would not be strictly required for TCA1 binding to the *petA* 5'UTR *in vivo* nor for translation activation, even though the latter process would be less efficient than in the presence of MCA1.

It is of note that both MCA1 and TCA1 can interact with themselves in yeast: MCA1 develops homomeric interactions via its N-terminal moiety, whereas TCA1 does so through its C-terminal region. In the absence of their other two partners from the *petA* gene expression system, each of the two proteins is

part of a protein complex of ~500 kD. These complexes could accommodate homotetramers of each factor, although the presence of additional proteins cannot be excluded. The ability of other *trans*-acting factors to oligomerize has been little investigated so far, with the exception of HCF152 that forms homodimers *in vitro* (Nakamura et al., 2003).

Very few examples of maturation/stability and translation factors acting on the same mRNA have been described to date. The NAC2 and RBP40 proteins that respectively govern the stability and the translation of the *psbD* transcript in *Chlamydomonas* interact as well, at least in the presence of the *psbD* mRNA (Schwarz et al., 2007), but their mode of action differs slightly from those of MCA1 and TCA1 since NAC2 seems to be strictly required for the recruitment of RBP40 onto the *psbD*

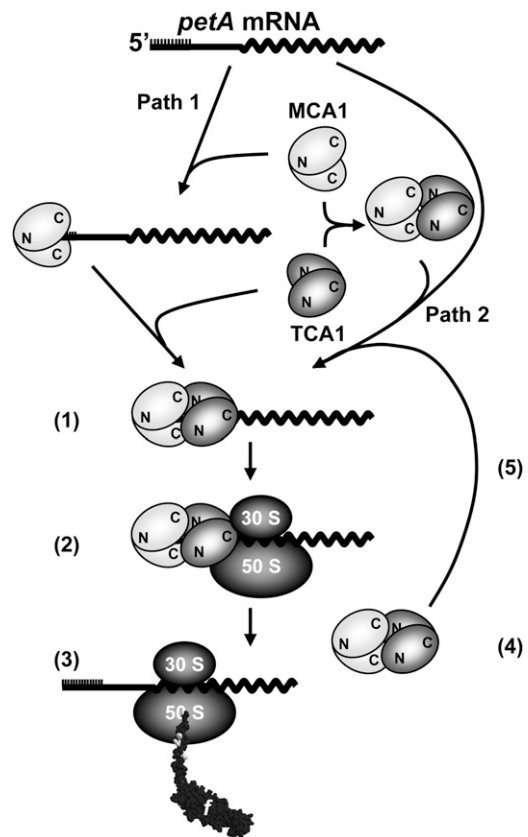


Figure 11. Working Model of the Biogenesis of the *petA* Gene Expression System.

MCA1 and TCA1 likely act *in vivo* as homo- and hetero-oligomers, whose formation would involve N- and C-terminal protein domains as indicated. MCA1 can bind to *petA* mRNA in the absence of TCA1 (Path 1) and also can interact with TCA1 in the absence of *petA* mRNA (Path 2). Both Paths 1 and 2 likely contribute *in vivo* to the formation of the ternary complex of ~600 kD (1) required for ribosome recruitment (2) and cytochrome *f* synthesis (3). Once translation is initiated, MCA1 and TCA1 would probably dissociate (4) from the translated mRNA and can be recycled for the formation of a new ternary complex (5) and new rounds of cytochrome *f* synthesis. Another interaction between MCA1 and unassembled cytochrome *f* is not shown in this figure but is detailed in Figure 12.

5'UTR and, therefore, for translation initiation (Ossenbühl and Nickelsen, 2000).

Whereas some RNA binding proteins are membrane embedded or show reversible association with the membrane (Zerges and Rochaix, 1998; Trebitsh et al., 2001; Ossenbühl et al., 2002; Zerges et al., 2002; Schult et al., 2007), MCA1 and TCA1, as most *trans*-acting factors (e.g., CRP1 [Fisk et al., 1999], NAC2 [Boudreau, 2000], MBB1 [Vaistij et al., 2000b], and TAB2 [Dauvillée et al., 2003]), are found in the chloroplast stroma. The functional significance of these contrasting distributions is still unclear but could reflect differences in the mode of action of nucleus-encoded factors: some may remain bound to polysomes, while others bind transiently to their target mRNA but dissociate once translation is initiated. As an example, NAC2 and RBP40 likely associate transiently with monosomes (Schwarz et al., 2007) but are not found in polysome fractions (Boudreau et al., 2000), suggesting that they are released from *psbD* transcript after translation initiation. We did not find, either, any evidence for the presence of MCA1 (or TCA1) in polysome fractions isolated according to Minai et al. (2006) from strains *mH* and *tF* (data not shown).

Unassembled Cytochrome *f* Induces MCA1 Degradation

In this article, we show that the degradation of MCA1 is regulated by its interaction with cytochrome *f*, namely, with the CES repressor domain that is located on its stroma-exposed C-terminal domain. This CES repressor domain drives MCA1 degradation when cytochrome *f* is in its unassembled state, i.e., transiently before cytochrome *b₆f* assembly in a wild-type context or for a longer time period when assembly is prevented, as is the case in a strain lacking SUIV, an assembly partner of

cytochrome *f*. Indeed, MCA1 accumulates to ~10-fold higher levels in the absence of cytochrome *f* C-terminal domain (strain *mH* $\{\Delta petA\}$ or *mH* $\{petA_{St}\}$) than in its presence (strain *mH*; Figure 6A). In the wild type, MCA1 is unstable, with a half-life in the hour range (Raynaud et al., 2007), but it becomes stable in the absence of cytochrome *f* (Figure 6B). Moreover, the degradation of MCA1 is triggered by the very same residues in the C-terminal tail that are responsible for CES (Choquet et al., 2003): MCA1 shows no notable degradation when the CES repressor domain is disrupted, either because of truncations (*mH* $\{f_{sol}\}$ or *mH* $\{f_{307St}\}$) or point mutations (*mH* $\{f_{307S}\}$ or *mH* $\{f\Delta K\}$; Figure 7B). The CES repressor motif should, however, be exposed by unassembled cytochrome *f* to promote MCA1 degradation: When its concentration is kept very low, as in strains expressing the unstable apocytochrome *f*, MCA1 is accumulated to higher levels than in the wild type (Figure 8A). By contrast, in assembly-defective mutants, such as the *mH* $\{\Delta petD\}$ strain, that accumulate long-lived unassembled CES repressor domains, MCA1 is less stable (Figure 8C) and hence is less accumulated (Figure 8B) than in the wild type, where the repressor domain is only transiently accessible before being shielded by the other subunits of the cytochrome *b₆f* complex.

Whether the interaction between MCA1 and the unassembled CES repressor domain is direct or indirect remains to be determined. If MCA1 binds to unassembled cytochrome *f*, it may become accessible to membrane-embedded proteases that have little access to the stromal soluble form of MCA1. This proteolytic disposal when membrane bound would explain why it is poorly found in membrane fractions.

The interaction of MCA1 with unassembled cytochrome *f* does not depend on its prior association with either TCA1 or the *petA* mRNA: MCA1 is still degraded, even in the absence of

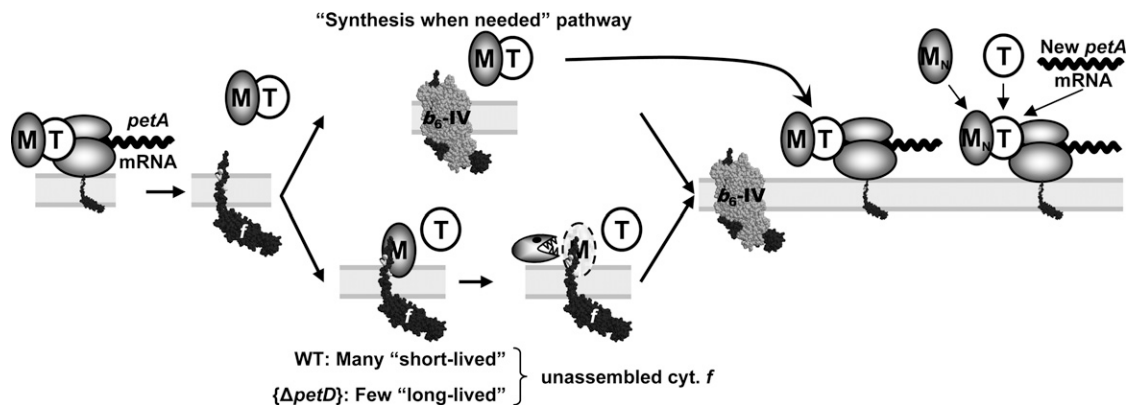


Figure 12. A Refined Model for the CES Process for Cytochrome *f*.

The biogenesis of the cytochrome *b₆f* complex in the wild type (WT) “synthesis when needed” pathway; see text. In strains with disrupted CES repressor domain, such as *f_{307St}*, MCA1 (M) cannot interact with unassembled cytochrome (cyt.) *f* (*f*) and is efficiently recycled for new rounds of *petA* mRNA translation (top part of the figure). In the wild type, free C-terminal tails of cytochrome *f* accumulate transiently before assembly (“many short-lived” unassembled cytochrome *f*; bottom part of the figure) and may interact with some MCA1 proteins that are thus targeted for degradation. By contrast, in strains defective for cytochrome *b₆f* complex assembly, such as $\Delta petD$, C-terminal tails of cytochrome *f*, although synthesized in reduced amount, are particularly long lived and would target most neighboring MCA1 for degradation (“few long-lived” unassembled cytochrome *f*; bottom part of the figure). The right side of the figure illustrates the formation of new ternary complexes following import of newly synthesized MCA1 (M_N). De novo biogenesis of cytochrome *f* in assembly-defective cytochrome *b₆f* mutants, such as $\{\Delta petD\}$, would mostly rely on these new ternary complexes. For the sake of clarity, MCA1 and TCA1 (T) are drawn as monomers, even if they are likely oligomeric in vivo (Figure 11).

TCA1, when cytochrome *f* is expressed from a chimeric gene whose 5' UTR is borrowed from the *atpA* gene. It should also be noted that TCA1, which is long lived in the chloroplast, is limiting for cytochrome *f* synthesis in complemented strains expressing low levels of this protein (Raynaud et al., 2007) but not in physiological conditions. By contrast, MCA1, which was previously shown to enhance translation (Loiselay et al., 2008), appears as a key player in the CES process for cytochrome *f*: A modified *petA* mRNA, even though stable in the absence of MCA1 because of a polyG track in its 5' UTR, is 10-fold less expressed than when MCA1 is present (Loiselay et al., 2008). This activation of translation by TCA1 in the absence of MCA1 is probably born by the C-terminal region of TCA1, which does not interact with MCA1 in the yeast two-hybrid system, but still complements *tca1* null mutants.

A New Model for the CES Process

Based on these new findings, we revisited our working model for the CES process driving cytochrome *f* production (Figure 12) to account for the proteolytic regulation of the amount of MCA1 available for cytochrome *f* translation as an exquisite nuclear control of a chloroplast-based regulation process.

In the wild type, cytochrome *f* synthesis will obey a "synthesis when needed" mechanism: Most newly synthesized cytochrome *f* is rapidly assembled into cytochrome *b₆f* complexes, preventing the binding of MCA1. The majority of MCA1 is therefore available for new rounds of translation (top part of the figure). The whole population of MCA1 follows this pathway in strains with disrupted CES repressor domain, such as *f₃₀₇St*, in which MCA1 cannot interact with cytochrome *f* and is very efficiently recycled for new rounds of translation, accounting for the 3-fold increased rate of *petA* mRNA translation.

In the wild type, a fraction of free C-terminal tail of cytochrome *f* that transiently accumulates before assembly would nevertheless interact with some MCA1 proteins that thus are targeted for degradation. De novo-synthesized MCA1 imported from the cytosol has to be recruited (right part of the figure) to compensate for MCA1 degradation (bottom part of the figure). This pathway would prevail when the synthesis of cytochrome *f* exceeds the rate of production of its assembly partners. In particular, when assembly of cytochrome *f* into the cytochrome *b₆f* complex is fully prevented, as in the $\{\Delta petD\}$ mutant lacking subunit IV, the long-lived C-terminal tail would target most neighboring MCA1 for degradation. Next rounds of cytochrome *f* synthesis would thus rely principally on de novo-synthesized MCA1, a process 10 times less efficient than reusing preexisting MCA1 as the wild type does.

However, the half-life of MCA1, in the hour range, is much longer than the time it takes for cytochrome *f* synthesis and assembly, in the minute range. In strain $\{\Delta petD\}$, MCA1, after interacting with unassembled cytochrome *f*, may be transiently trapped, either on the long-lasting unassembled cytochrome *f* or within oligomeric forms, such as the TCA1-MCA1 complexes observed in our size exclusion chromatography experiments. These forms should be poorly competent for translation initiation, explaining why the steady state concentration of MCA1 in assembly-defective strains is less reduced (2- to 3-fold) than the rate of cytochrome *f* synthesis (10-fold) when compared with

the wild-type situation. It is worth noting that, although 3 times more MCA1 accumulates in *tca1* mutants than in the wild type, the accumulation of the *petA* transcript is nevertheless reduced 5-fold, suggesting that MCA1 is present mostly as homo-oligomers that poorly contribute to *petA* mRNA stabilization.

Altogether, our results further substantiate the regulatory role of nucleus-encoded factors in the expression of their organelle target genes. The regulatory function of MCA1 in the fine-tuning of cytochrome *f* synthesis involves a regulated proteolysis, triggered by its interaction with unassembled cytochrome *f*. Whether this mechanism can be generalized to other factors controlling the expression of other CES proteins remains to be determined.

METHODS

Strains, Growth Conditions, and Crosses

Wild-type (derived from 137c), mutant, and complemented strains of *Chlamydomonas reinhardtii* were grown in Tris-acetate-phosphate (TAP) medium, pH 7.2 (Harris, 1989), supplemented with 1% sorbitol when growing *cw15* (cell wall-less) strains, under continuous light (5 to 10 $\mu\text{E}\cdot\text{m}^{-2}\cdot\text{s}^{-1}$) on a rotatory shaker (120 rpm). Strains *tca1-8*, *tca1-8 cw15*, and *mca1-2 cw15*, as well as the complemented derivatives (*tF*, *tF cw15*, and *mH cw15*; the two latter strains used for the isolation of intact chloroplasts and the preparation of stromal extracts) have been described by (Raynaud et al., 2007). The complemented strain expressing TCA1-FI was the most right-located strain (indicated by an asterisk in Figure 3A from Raynaud et al. [2007]). The strain *mca1-6*, carrying a new allele of *MCA1*, is briefly described below and in Supplemental Figure 1 online. It was used as recipient strain for nuclear transformation experiments with plasmid *plgMCA1-HA* linearized by digestion with *XbaI* (Raynaud et al., 2007) to generate the complemented strain *mH*. We also used the chloroplast mutants *ccsA-B6* (Xie et al., 1998), *f₃₀₇S* (Choquet et al., 2003), and $\Delta petD$ (Kuras and Wollman, 1994).

In this work, strains are named by their genotype. By convention, *t* indicates a strain carrying the *tca1-8* mutant allele at the *TCA1* locus, whereas *m* denotes a mutated *MCA1* locus (either the *mca1-2* allele in cell wall-less strains carrying the *cw15* mutation or the *mca1-6* allele in cell-walled strains). *F* indicates that the *tca1-8* mutation had been complemented by a Flag-tagged version of *TCA1*, whereas *H* indicates the complementation of either *mca1* allele by the HA-tagged version of *MCA1*. As an example, the *mHt* strain expresses the tagged version of *MCA1* in the absence of *TCA1*. Chloroplast genotype, when relevant, follows the nuclear genotype and is written between brackets. The construction of the strains used in this study is described in Tables 1 and 2.

Crosses, described in Table 1, were performed according to Harris (1989). We used a genetic strategy to compare the expression of the tagged versions of *MCA1* and *TCA1* between different strains in Figures 5A and 5B. Indeed, we consistently observed in crosses involving *mH* or *tF* strains that the expression of the transgene remains constant (with variations below 15% of the level observed in the parental strain) in progeny with a similar genotype. Compare, for example, the parental strain *mH* to the *mH* progeny of the cross *mH* \times *mt* in Figure 5C or the *tF* parental strain to the *tF* progeny from the cross *tF* \times *mt* in Figure 5A. After transformation, the expression level of a transgene strongly depends on the site of the insertion but appears poorly sensitive to the genetic background, shuffled during the cross.

Description of the *mca1-6* Mutation

Strain *mca1-6* (CAL015.01.25), kindly provided by Rachel Dent, belongs to a library of mutants generated by random insertion of the *b_{le}* cassette

(Dent et al., 2005). This mutant requires acetate in the medium for growth, lacks accumulation of the *petA* mRNA (see Supplemental Figure 1B online), and could be complemented by the *MCA1* gene, leading to strain *mH* (see Supplemental Figure 1A online). The mutation is tightly linked to the insertion of the *ble* cassette conferring resistance to up to 10 $\mu\text{g}\cdot\text{mL}^{-1}$ of zeocin. This allowed following the segregation of the mutation when analyzing the crosses listed in Table 1. The *ble* cassette is probably inserted in the 3' part of the *MCA1* gene, as no PCR product could be amplified with primers *MCA1cod3* and *MCA1rev3* (primers used in this work are listed in Supplemental Table 1 online), which respectively hybridize to the downstream third of the coding sequence and to the 3'UTR. The mutation is nevertheless not a deletion, as the reversion frequency, although very low, is not null.

Construction and Nucleic Acid Manipulation

Standard nucleic acid manipulations were performed according to Sambrook et al. (1989).

The *petA*_{Stop} Construct

The *pWF*_{Stop} construct contains a mutated *petA* gene that cannot be translated since the *petA* initiation codon was substituted by a Stop codon (TAG). It was created by a two-step PCR procedure (Higuchi, 1990): two pairs of primers, *petACodMS/petA*_{Stop}Rev and *petA*_{Stop}Cod/*petA*Rev2, allowed amplification from the template plasmid *pWF* (Kuras and Wollman, 1994) of two partially overlapping fragments that were mixed and used as templates in a third PCR with the external primers *petACodMS* and *petA*Rev2. The final amplicon, carrying the Stop codon, was digested by *Bgl*III and *Hind*III, two restriction sites on either side of the mutation, and cloned into plasmid *pWF* digested with the same enzymes to create plasmid *pWF*_{Stop}. The 5'*psaA-aadA-3'rbcl* cassette (Wostrikoff et al., 2004) was then inserted at the *Hinc*II blunt site, upstream of and in reverse orientation with respect to the *petA* coding sequence. This plasmid, *pWF*_{Stop} K, was sequenced before transformation in *C. reinhardtii*.

Construction of 5'*atpA*-Driven *petA* Genes

We first associated the 5'*dAf* chimera with an *aadA* cassette conferring resistance to the antibiotics spectinomycin and streptomycin to allow selection of transformed strains. The 4214-bp fragment isolated from plasmid *pAFFF* (Choquet et al., 1998), digested with *Acc*I and *Sca*I, was ligated with the 5434- and 5565-bp fragments recovered from plasmids *pWFB* ATG12 (Rimbault et al., 2000) and *p*_{f₃₀₇S} (Choquet et al., 2003) digested with the same enzyme to yield plasmids *p5'dAf*K and *p5'dAf*₃₀₇S.

Cloning of *MCA1*, *TCA1*, and *MBB1* cDNAs in Yeast Two-Hybrid Vectors

MCA1. A 568-bp fragment encompassing the N terminus of *MCA1* was amplified with primers *MCA1_EcoRI_dir* and *MCA1_AscI_SalI_rev* from the template cDNA clone CL01e04, obtained from the Kazusa DNA Research Institute (<http://www.kazusa.or.jp/en/plant/>), digested with *Eco*RI and *Sal*I, and cloned into the corresponding sites of vectors *pGAD424* and *pGBT-9* (Clontech) to generate the *pAD-5'MCA1* and *pBD-5'MCA1* plasmids, respectively. Plasmid CL01e04 was then digested with *Asc*I and *Nsi*I to recover the last 2681 bp of the *MCA1* cDNA, and this fragment was cloned into vectors *pAD-5'MCA1* and *pBD-5'MCA1* digested with *Asc*I and *Pst*I to yield plasmids *pAD-MCA1* and *pBD-MCA1*. The *NMCA1* constructs were generated by digestion

of plasmids *pAD-MCA1* and *pBD-MCA1* with *Sal*I and *Bam*HI, Klenow treatment, and self-ligation.

TCA1. A 409-bp fragment encompassing nucleotides 814 to 1214 of the *TCA1* coding sequence was PCR amplified using primers *TCA1_EcoRI_814_dir* and *TCA1_1212_rev* and the cDNA clone HCL001 h11_r, obtained from the Kazusa DNA Research Institute, as a template. The amplicon contained a *Sfi*I site, while the *TCA1_EcoRI_814_dir* primer introduced an *Eco*RI site at its 5' end and was digested by these two enzymes. A 2560-bp fragment of the *TCA1* cDNA encompassing the C terminus of the protein was isolated from plasmid HCL001 h11_r digested by *Sfi*I and *Xho*I. The two fragments were inserted by a trimolecular ligation into vectors *pGAD424* and *pGBT9* digested with *Eco*RI and *Sal*I to yield plasmids *pAD-CTCA1* and *pBD-CTCA1*, respectively.

To clone the full-length *TCA1* cDNA into *pGAD424* and *pGBT-9* vectors, the first 1212 bp of *TCA1* were amplified with primers *TCA1_EcoRV_dir* and *TCA1_1212_rev* and digested with *Eco*RV and *Sfi*I. The last 2560 bp of the *TCA1* cDNA were isolated as above by digestion of plasmid HCL001 h11_r with *Sfi*I and *Xho*I. These two fragments were coligated into the *Sma*I and *Sal*I sites of vectors *pGAD424* and *pGBT9* to generate plasmids *pAD-TCA1* and *pBD-TCA1*, respectively. To create constructs *pAD-NTCA1* and *pBD-NTCA1* that only contain the first 1173 bp of the *TCA1* coding sequence, plasmids *pAD-TCA1* and *pBD-TCA1* were digested with *Sfi*I and *Nde*I, blunt-ended with Klenow and T4 DNA polymerase and self-ligated.

MBB1. A 410-bp fragment encompassing the N terminus of the *MBB1* gene, PCR amplified with primers *MBB1_dir_EcoRI-1* and *MBB1_rev_410* from template *pKS-MBB1* (Vaistij et al., 2000b) was digested by *Eco*RI and *Bam*HI. The last 1572 bp of *MBB1* were obtained by digesting the same plasmid *pKS-MBB1* with *Bam*HI and *Sal*I. These two fragments were cloned between the *Eco*RI and *Sal*I sites of vectors *pGAD424* and *pGBT-9* to yield clones *pAD-MBB1* and *pBD-MBB1*, respectively.

Two-Hybrid Assays in Yeast

Yeast two-hybrid assays were performed in the PJ69-a strain (Leu⁻, Trp⁻, Gal4-His, and Gal4-Ade) that expresses the HIS2 and ADE genes under the control of the Gal4-UAS. Interactions between proteins of interest reconstitute a functional Gal4 transcription factor and therefore restore prototrophy for His and adenine. This was tested by assessing growth of double transformants on two media of increasing stringency: minimum medium depleted for His and supplemented with 3-AT (a competitive inhibitor of HIS2) or depleted for both His and adenine.

For yeast transformation, cells were grown overnight in complete YPDA medium. A 1-mL culture was centrifuged at 1000g for 1 min; cells were washed with 1 mL deionized water and resuspended in 20 μL deionized water in the presence of 50 μg of salmon sperm DNA and 1 μg of each plasmid. After addition of 200 μL PEG (PEG-4000 50%, 0.1 M lithium acetate, and 1 \times TE) and 20 μL DMSO, cells were incubated for 15 min at 30°C with shaking and then at 42°C for 15 min. After addition of 1 mL water, cells were harvested by centrifugation, washed once with 1 mL water, resuspended in 100 μL water, and plated on minimal medium lacking Leu and Trp since cotransformation with both *pGAD424* and *pGBT-9* derivatives restores the prototrophy for Leu and Trp.

Double transformants were resuspended in water to an OD₆₀₀ of 1, and 10 μL of serial dilutions were spotted on the various selective media.

Transformation Experiments

Nuclear transformation of *mca1-6*, *tca1-8*, and *mtF* mutant strains was performed by electroporation, as described by Raynaud et al. (2007), with the following parameters: 10 $\mu\text{F}/1200\text{ V}\cdot\text{cm}^{-1}$. Transformants were

selected for phototrophy on minimum medium (Harris, 1989) under high light ($200 \mu\text{E}\cdot\text{m}^{-2}\cdot\text{s}^{-1}$).

Chloroplast transformation experiments, listed in Table 2, were performed by tungsten particle bombardment (Boynton et al., 1988) as described earlier (Kuras and Wollman, 1994). For each transformation, at least four independent transformants were analyzed. Phenotypic variations between independent transformants proved negligible.

RNA Isolation and Analysis

RNA extraction and RNA gel blot analysis were performed as described by Drapier et al. (2002) with probes derived from coding sequences (Eberhard et al., 2002).

Protein Preparation, Separation, and Analysis

Protein isolation, separation, and immunoblot analyses were performed on exponentially growing cells (2×10^6 cells·mL⁻¹) as described by Kuras and Wollman (1994). All immunoblots were repeated at least twice and performed on three independent transformants. Cell extracts were loaded on an equal chlorophyll basis, unless otherwise specified. Antibodies against the β -subunit of F1/CF1, the OEE2 subunit from the photosystem II oxygen-evolving complex, cytochrome *f*, Nac2, and GrpE have been described (Lemaire et al., 1986; de Vitry et al., 1989; Kuras and Wollman, 1994; Boudreau et al., 2000; Schroda et al., 2001). TCA1-FI and MCA1-HA were detected by ECL using monoclonal antibodies, anti-Flag M2 (Sigma-Aldrich) and anti-HA.11 (Covance), and horseradish peroxidase-conjugated antibody against mouse IgG (Promega). Their accumulation (normalized to that of the F1 β subunit from the mitochondrial ATP synthase as an internal standard) was, when required, quantified from scanned films with the Image-Quant software (Molecular Dynamics), according to Raynaud et al. (2007). Cytochrome *f* accumulation, normalized to that of the β -subunit of the mitochondrial ATP synthase as an internal standard, was quantified from phosphor imager scans of immunoblots revealed with ¹²⁵I protein A or by ECL, using the ImageQuant software, as described by Choquet et al. (2003) and Raynaud et al. (2007).

Immunochase was performed on whole cells grown in TAP medium (2×10^6 cell·mL⁻¹), supplemented at $t = 0$ with either cycloheximide (final concentration: $10 \mu\text{g}\cdot\text{mL}^{-1}$), lincomycin (final concentration $500 \mu\text{g}\cdot\text{mL}^{-1}$), or both. At the indicated time points, aliquots were removed, briefly chilled on ice, and processed as described above before loading on gels.

Stromal Preparations

Chloroplasts from cell wall-deficient strains were isolated according to Zerges et al. (2002). After limited cell lysis with 1% (w/v) saponin, extracts were loaded on a discontinuous (45/75%) Percoll gradient. Intact chloroplasts were recovered at the interface between the 45 and 75% Percoll solutions and washed once with isotonic buffer (0.3 M sorbitol, 5 mM MgCl₂, and 10 mM Tricine, pH 7.8). To prepare stromal fractions, intact chloroplasts were osmotically lysed in hypotonic buffer (10 mM Tricine, pH 7.8; and $5\times$ Roche protease inhibitors) by repeated pipetting. Broken chloroplasts were then centrifuged at $16,000g$ for 10 min at 4°C, and the concentration of stromal proteins in the supernatant was estimated by the Bradford method (Bio-Rad Quick Start Bradford Dye Reagent).

Gel Filtration Experiments on Stromal or Soluble Extracts

A 600-mL culture at 2×10^6 cells·mL⁻¹ was centrifuged and resuspended in 3 mL of breaking buffer (5 mM HEPES-KOH, pH 7.8, 20 mM KCl, 10% glycerol, $0.5 \text{ g}\cdot\text{L}^{-1}$ heparin, and $5\times$ Roche protease inhibitors). Cells were broken with a French press at 6000 p.s.i. and centrifuged at $346,000g$ for 20 min to pellet the membranes and debris. Two mL of the supernatant

or of stromal extracts were loaded on a Sephacryl S500 column (GE Healthcare), and elution was performed at a rate of $700 \mu\text{L}\cdot\text{min}^{-1}$, at 4°C, with a buffer containing 80 mM Tricine-KOH, pH 7.8, 200 mM KCl, 10 mM EDTA, 20 mM ϵ -aminocaproic acid, and $0.1\times$ Roche protease inhibitors. Sixteen 5-mL fractions, eluted 40 mL after injection, were collected and concentrated by centrifugation on Amicon Ultra-15 filter units (cutoff: 50 kD) at $4500g$ for 20 min. Fraction volumes were then adjusted to $500 \mu\text{L}$, out of which $80 \mu\text{L}$ were loaded on 12% acrylamide gels containing 8 M urea. Fraction 16 (smallest molecular mass) lacked any protein of interest and was not loaded on the gels. For RNase treatments, stromal preparations, prepared in breaking buffer lacking heparin, were incubated at 4°C with $2500 \text{ units}\cdot\text{mL}^{-1}$ of both RNase I and RNase A for 45 min under gentle and continuous shaking, prior to loading on the column.

Coimmunoprecipitations

A 400-mL culture at 2×10^6 cells·mL⁻¹ was centrifuged and resuspended in 2 mL of breaking buffer (20 mM HEPES-KOH, pH 7.2, 150 mM NaCl, 10 mM KCl, 1 mM MgCl₂, 10% glycerol, and $2\times$ Roche protease inhibitors). Cells, broken by a French press at 6000 p.s.i., were centrifuged at $34,000g$ for 30 min to pellet membranes and debris. Five hundred microliters of the supernatant and $20 \mu\text{L}$ of beads coupled to anti-HA (HA11 Affinity Matrix; Covance) or anti-Flag (Flag immunoprecipitation kit; Sigma-Aldrich) antibodies were incubated for 1 h at 4°C, after which beads were washed three times with washing buffer (150 mM NaCl, 20 mM HEPES-KOH, pH 7.2, and 10% glycerol supplemented with $1\times$ Roche protease inhibitors) and two more times with 10 mM Tris-HCl, pH 7.5. Bound proteins were detached by incubation for 1 min in 2% SDS at 95°C and analyzed by immunoblots.

Two-Step Centrifugation Procedure

The 400-mL cultures of *mH* and *tF* strains at 2×10^6 cells·mL⁻¹ were centrifuged and resuspended in 3 mL of breaking buffer (5 mM HEPES-KOH, pH 7.8, 20 mM KCl, 10% glycerol, $0.5 \text{ g}\cdot\text{L}^{-1}$ heparin, and $5\times$ Roche protease inhibitors). Cells, broken by a French press (6000 p.s.i.), were centrifuged at $21,000g$ for 5 min to remove unbroken cells, starch, and large debris. One milliliter of the supernatant (Extract E) was layered on top of a 1-mL 1.5 M sucrose cushion and ultracentrifuged at $272,000g$ for 30 min, giving rise to supernatant Sn, membrane fraction Mb, sucrose cushion C, and pellet P. All fractions were adjusted to 1 mL with breaking buffer. An aliquot of the whole-cell extract E was loaded on gel, after spectroscopic determination of chlorophyll concentration, together with equal volumes of fractions Sn and Mb, and analyzed by immunoblot. Cytochrome *f* and GrpE were used as membrane and soluble markers, respectively.

Accession Numbers

Sequence data from this article can be found in the GenBank/EMBL data libraries under the following accession numbers: *TCA1*, EF503563.1; *MCA1*, AF330231.1; *MBB1*, AJ296291.1; *NAC2*, AJ271460.1; and *petA*, FJ423446.1.

Supplemental Data

The following materials are available in the online version of this article.

Supplemental Figure 1. Characterization of the *mca1-6* and *mH* Strains.

Supplemental Figure 2. Accumulation of Cytochrome *f*, Detected by Immunoblots in the Wild Type and in the *CTCA1* Strain (the *tca1-8* Mutant Complemented with the C-Terminal Domain of TCA1).

Supplemental Table 1: Oligonucleotides Used in This Work.

ACKNOWLEDGMENTS

We thank R. Dent for her kind gift of the *mca1-6* strain, J.-D. Rochaix for providing antibody against the NAC2 protein and plasmid MBB1-pKS, J. Nickelsen, C. Schwarz, D. Picot, C. Breyton, D. Charvolin, S. Masscheleyn, and B. Miroux for their help with size exclusion chromatography experiments, and B. Bailleul, K. Wostrikoff, D. Drapier, S. Eberhard, and R. Kuras for stimulating discussions and/or critical reading of the manuscript. This work was supported by Centre National de la Recherche Scientifique/Université Pierre et Marie Curie, Unité Mixte de Recherche 7141, and the European Community, SunBioPath contract FP7-KBBE-2009-3-02. C.R. and A.B. were "Attachées Temporaires d'Enseignement et de Recherche" at Université Pierre et Marie Curie.

Received July 15, 2010; revised November 26, 2010; accepted December 7, 2010; published January 7, 2011.

REFERENCES

- Ackerman, S.H., and Tzagoloff, A.** (2005). Function, structure, and biogenesis of mitochondrial ATP synthase. *Prog. Nucleic Acid Res. Mol. Biol.* **80**: 95–133.
- Anderson, S., et al.** (1981). Sequence and organization of the human mitochondrial genome. *Nature* **290**: 457–465.
- Auchincloss, A.H., Zerges, W., Perron, K., Girard-Bascou, J., and Rochaix, J.-D.** (2002). Characterization of Tbc2, a nucleus-encoded factor specifically required for translation of the chloroplast *psbC* mRNA in *Chlamydomonas reinhardtii*. *J. Cell Biol.* **157**: 953–962.
- Balczun, C., Bunse, A., Hahn, D., Bennoun, P., Nickelsen, J., and Kück, U.** (2005). Two adjacent nuclear genes are required for functional complementation of a chloroplast trans-splicing mutant from *Chlamydomonas reinhardtii*. *Plant J.* **43**: 636–648.
- Barkan, A., and Goldschmidt-Clermont, M.** (2000). Participation of nuclear genes in chloroplast gene expression. *Biochimie* **82**: 559–572.
- Boudreau, E., Nickelsen, J., Lemaire, S.D., Ossenhübl, F., and Rochaix, J.-D.** (2000). The *Nac2* gene of *Chlamydomonas* encodes a chloroplast TPR-like protein involved in *psbD* mRNA stability. *EMBO J.* **19**: 3366–3376.
- Boynton, J.E., et al.** (1988). Chloroplast transformation in *Chlamydomonas* with high velocity microprojectiles. *Science* **240**: 1534–1538.
- Cardol, P., and Remacle, C.** (2009). The mitochondrial genome. In *The Chlamydomonas Source Book*, 2nd ed, Vol. 2, E.E. Harris, D.B. Stern, and G. Whitman, eds (New York, London: Academic Press, Elsevier), pp. 445–469.
- Choquet, Y., and Wollman, F.-A.** (2002). Translational regulations as specific traits of chloroplast gene expression. *FEBS Lett.* **529**: 39–42.
- Choquet, Y., and Wollman, F.-A.** (2009). The CES process. In *The Chlamydomonas Source Book*, 2nd ed, Vol. 2, E.E. Harris, D.B. Stern, and G. Whitman, eds (New York, London, Amsterdam: Academic Press, Elsevier), pp. 1027–1064.
- Choquet, Y., Stern, D.B., Wostrikoff, K., Kuras, R., Girard-Bascou, J., and Wollman, F.-A.** (1998). Translation of cytochrome *f* is autoregulated through the 5' untranslated region of *petA* mRNA in *Chlamydomonas* chloroplasts. *Proc. Natl. Acad. Sci. USA* **95**: 4380–4385.
- Choquet, Y., Zito, F., Wostrikoff, K., and Wollman, F.-A.** (2003). Cytochrome *f* translation in *Chlamydomonas* chloroplast is autoregulated by its carboxyl-terminal domain. *Plant Cell* **15**: 1443–1454.
- Dauvillée, D., Stampacchia, O., Girard-Bascou, J., and Rochaix, J.-D.** (2003). Tab2 is a novel conserved RNA binding protein required for translation of the chloroplast *psaB* mRNA. *EMBO J.* **22**: 6378–6388.
- Dent, R.M., Haglund, C.M., Chin, B.L., Kobayashi, M.C., and Niyogi, K.K.** (2005). Functional genomics of eukaryotic photosynthesis using insertional mutagenesis of *Chlamydomonas reinhardtii*. *Plant Physiol.* **137**: 545–556.
- de Vitry, C., Olive, J., Drapier, D., Recouvreur, M., and Wollman, F.A.** (1989). Posttranslational events leading to the assembly of photosystem II protein complex: A study using photosynthesis mutants from *Chlamydomonas reinhardtii*. *J. Cell Biol.* **109**: 991–1006.
- de Zamaroczy, M., and Bernardi, G.** (1986). The primary structure of the mitochondrial genome of *Saccharomyces cerevisiae*—A review. *Gene* **47**: 155–177.
- Drager, R.G., Girard-Bascou, J., Choquet, Y., Kindle, K.L., and Stern, D.B.** (1998). In vivo evidence for 5'→3' exoribonuclease degradation of an unstable chloroplast mRNA. *Plant J.* **13**: 85–96.
- Drapier, D., Girard-Bascou, J., Stern, D.B., and Wollman, F.-A.** (2002). A dominant nuclear mutation in *Chlamydomonas* identifies a factor controlling chloroplast mRNA stability by acting on the coding region of the *atpA* transcript. *Plant J.* **31**: 687–697.
- Drapier, D., Rimbault, B., Vallon, O., Wollman, F.-A., and Choquet, Y.** (2007). Intertwined translational regulations set uneven stoichiometry of chloroplast ATP synthase subunits. *EMBO J.* **26**: 3581–3591.
- Eberhard, S., Drapier, D., and Wollman, F.-A.** (2002). Searching limiting steps in the expression of chloroplast-encoded proteins: relations between gene copy number, transcription, transcript abundance and translation rate in the chloroplast of *Chlamydomonas reinhardtii*. *Plant J.* **31**: 149–160.
- Fisk, D.G., Walker, M.B., and Barkan, A.** (1999). Molecular cloning of the maize gene *crp1* reveals similarity between regulators of mitochondrial and chloroplast gene expression. *EMBO J.* **18**: 2621–2630.
- Fontanesi, F., Soto, I.C., and Barrientos, A.** (2008). Cytochrome *c* oxidase biogenesis: New levels of regulation. *IUBMB Life* **60**: 557–568.
- Foury, F., Roganti, T., Lecrenier, N., and Purnelle, B.** (1998). The complete sequence of the mitochondrial genome of *Saccharomyces cerevisiae*. *FEBS Lett.* **440**: 325–331.
- Fox, T.D.** (1996). *Genetics of Mitochondrial Translation*. (Cold Spring Harbor, NY: Cold Spring Harbor Laboratory Press).
- Fromont-Racine, M., Rain, J.C., and Legrain, P.** (1997). Toward a functional analysis of the yeast genome through exhaustive two-hybrid screens. *Nat. Genet.* **16**: 277–282.
- Green-Willms, N.S., Butler, C.A., Dunstan, H.M., and Fox, T.D.** (2001). Pet111p, an inner membrane-bound translational activator that limits expression of the *Saccharomyces cerevisiae* mitochondrial gene COX2. *J. Biol. Chem.* **276**: 6392–6397.
- Haffter, P., and Fox, T.D.** (1992). Suppression of carboxy-terminal truncations of the yeast mitochondrial mRNA-specific translational activator PET122 by mutations in two new genes, *MRP17* and *PET127*. *Mol. Gen. Genet.* **235**: 64–73.
- Haffter, P., McMullin, T.W., and Fox, T.D.** (1991). Functional interactions among two yeast mitochondrial ribosomal proteins and an mRNA-specific translational activator. *Genetics* **127**: 319–326.
- Harris, E.H.** (1989). *The Chlamydomonas Source Book: A Comprehensive Guide to Biology and Laboratory Use*. (San Diego, CA: Academic Press).
- Hattori, M., and Sugita, M.** (2009). A moss pentatricopeptide repeat protein binds to the 3' end of plastid *clpP* pre-mRNA and assists with mRNA maturation. *FEBS J.* **276**: 5860–5869.
- Herrin, D.L., and Nickelsen, J.** (2004). Chloroplast RNA processing and stability. *Photosynth. Res.* **82**: 301–314.
- Higuchi, R.** (1990). Recombinant PCR. In *PCR Protocols: A Guide to Methods and Applications*, D.H. Gelfand, M.A. Innis, J.J. Sninsky, and T.J. White, eds (New York/London/Amsterdam: Academic Press, Elsevier), pp. 177–183.
- Islas-Osuna, M.A., Ellis, T.P., Marnell, L.L., Mittelmeier, T.M., and**

- Dieckmann, C.L.** (2002). Cbp1 is required for translation of the mitochondrial cytochrome *b* mRNA of *Saccharomyces cerevisiae*. *J. Biol. Chem.* **277**: 37987–37990.
- Keeling, P.J.** (2009). Role of horizontal gene transfer in the evolution of photosynthetic eukaryotes and their plastids. *Methods Mol. Biol.* **532**: 501–515.
- Klinkert, B., Elles, I., and Nickelsen, J.** (2006). Translation of chloroplast *psbD* mRNA in *Chlamydomonas* is controlled by a secondary RNA structure blocking the AUG start codon. *Nucleic Acids Res.* **34**: 386–394.
- Krause, K., Lopes de Souza, R., Roberts, D.G., and Dieckmann, C.L.** (2004). The mitochondrial message-specific mRNA protectors Cbp1 and Pet309 are associated in a high-molecular weight complex. *Mol. Biol. Cell* **15**: 2674–2683.
- Kuchka, M.R., Goldschmidt-Clermont, M., van Dillewijn, J., and Rochaix, J.-D.** (1989). Mutation at the *Chlamydomonas* nuclear NAC2 locus specifically affects stability of the chloroplast *psbD* transcript encoding polypeptide D2 of PS II. *Cell* **58**: 869–876.
- Kuras, R., Büschlen, S., and Wollman, F.-A.** (1995b). Maturation of pre-apocytochrome *f* *in vivo*. A site-directed mutagenesis study in *Chlamydomonas reinhardtii*. *J. Biol. Chem.* **270**: 27797–27803.
- Kuras, R., and Wollman, F.-A.** (1994). The assembly of cytochrome *b₆/f* complexes: An approach using genetic transformation of the green alga *Chlamydomonas reinhardtii*. *EMBO J.* **13**: 1019–1027.
- Kuras, R., Wollman, F.-A., and Joliot, P.** (1995a). Conversion of cytochrome *f* to a soluble form *in vivo* in *Chlamydomonas reinhardtii*. *Biochemistry* **34**: 7468–7475.
- Lemaire, C., Girard-Bascou, J., Wollman, F.-A., and Bennoun, P.** (1986). Studies on the cytochrome *b₆f* complex. I. Characterization of the complex subunits in *Chlamydomonas reinhardtii*. *Biochim. Biophys. Acta* **851**: 229–238.
- Loiselay, C., Gumpel, N.J., Girard-Bascou, J., Watson, A.T., Purton, S., Wollman, F.-A., and Choquet, Y.** (2008). Molecular identification and function of cis- and trans-acting determinants for *petA* transcript stability in *Chlamydomonas reinhardtii* chloroplasts. *Mol. Cell. Biol.* **28**: 5529–5542.
- McMullin, T.W., Haffter, P., and Fox, T.D.** (1990). A novel small-subunit ribosomal protein of yeast mitochondria that interacts functionally with an mRNA-specific translational activator. *Mol. Cell. Biol.* **10**: 4590–4595.
- Martin, W., Stoebe, B., Goremykin, V., Hapsmann, S., Hasegawa, M., and Kowallik, K.V.** (1998). Gene transfer to the nucleus and the evolution of chloroplasts. *Nature* **393**: 162–165.
- Merendino, L., Perron, K., Rahire, M., Howald, I., Rochaix, J.-D., and Goldschmidt-Clermont, M.** (2006). A novel multifunctional factor involved in trans-splicing of chloroplast introns in *Chlamydomonas*. *Nucleic Acids Res.* **34**: 262–274.
- Minai, L., Wostrikoff, K., Wollman, F.A., and Choquet, Y.** (2006). Chloroplast biogenesis of photosystem II cores involves a series of assembly-controlled steps that regulate translation. *Plant Cell* **18**: 159–175.
- Monod, C., Goldschmidt-Clermont, M., and Rochaix, J.-D.** (1992). Accumulation of chloroplast *psbB* RNA requires a nuclear factor in *Chlamydomonas reinhardtii*. *Mol. Gen. Evol.* **231**: 449–459.
- Nakamura, T., Meierhoff, K., Westhoff, P., and Schuster, G.** (2003). RNA-binding properties of HCF152, an *Arabidopsis* PPR protein involved in the processing of chloroplast RNA. *Eur. J. Biochem.* **270**: 4070–4081.
- Naithani, S., Saracco, S.A., Butler, C.A., and Fox, T.D.** (2003). Interactions among COX1, COX2, and COX3 mRNA-specific translational activator proteins on the inner surface of the mitochondrial inner membrane of *Saccharomyces cerevisiae*. *Mol. Biol. Cell* **14**: 324–333.
- Nickelsen, J., Fleischmann, M., Boudreau, E., Rahire, M., and Rochaix, J.-D.** (1999). Identification of cis-acting RNA leader elements required for chloroplast *psbD* gene expression in *Chlamydomonas*. *Plant Cell* **11**: 957–970.
- Nickelsen, J., van Dillewijn, J., Rahire, M., and Rochaix, J.-D.** (1994). Determinants for stability of the chloroplast *psbD* RNA are located within its short leader region in *Chlamydomonas reinhardtii*. *EMBO J.* **13**: 3182–3191.
- Ossenbühl, F., Hartmann, K., and Nickelsen, J.** (2002). A chloroplast RNA binding protein from stromal thylakoid membranes specifically binds to the 5' untranslated region of the *psbA* mRNA. *Eur. J. Biochem.* **269**: 3912–3919.
- Ossenbühl, F., and Nickelsen, J.** (2000). cis- and trans-acting determinants for translation of *psbD* mRNA in *Chlamydomonas reinhardtii*. *Mol. Cell. Biol.* **20**: 8134–8142.
- Perron, K., Goldschmidt-Clermont, M., and Rochaix, J.-D.** (1999). A factor related to pseudouridine synthases is required for chloroplast group II intron trans-splicing in *Chlamydomonas reinhardtii*. *EMBO J.* **18**: 6481–6490.
- Perron, K., Goldschmidt-Clermont, M., and Rochaix, J.-D.** (2004). A multiprotein complex involved in chloroplast group II intron splicing. *RNA* **10**: 704–711.
- Pfzal, J., Bayraktar, O.A., Prikryl, J., and Barkan, A.** (2009). Site-specific binding of a PPR protein defines and stabilizes 5' and 3' mRNA termini in chloroplasts. *EMBO J.* **28**: 2042–2052.
- Raynaud, C., Loiselay, C., Wostrikoff, K., Kuras, R., Girard-Bascou, J., Wollman, F.-A., and Choquet, Y.** (2007). Evidence for regulatory function of nucleus-encoded factors on mRNA stabilization and translation in the chloroplast. *Proc. Natl. Acad. Sci. USA* **104**: 9093–9098.
- Rimbault, B., Esposito, D., Drapier, D., Choquet, Y., Stern, D., and Wollman, F.-A.** (2000). Identification of the initiation codon for the *atpB* gene in *Chlamydomonas* chloroplasts excludes translation of a precursor form of the β subunit of the ATP synthase. *Mol. Gen. Evol.* **264**: 486–491.
- Sambrook, J., Fritsch, E.F., and Maniatis, T.** (1989). *Molecular Cloning*. (Cold Spring Harbor, NY: Cold Spring Harbor Laboratory Press).
- Schroda, M., Vallon, O., Whitelegge, J.P., Beck, C.F., and Wollman, F.-A.** (2001). The chloroplastic GrpE homolog of *Chlamydomonas*: Two isoforms generated by differential splicing. *Plant Cell* **13**: 2823–2839.
- Schult, K., Meierhoff, K., Paradies, S., Töller, T., Wolff, P., and Westhoff, P.** (2007). The nuclear-encoded factor HCF173 is involved in the initiation of translation of the *psbA* mRNA in *Arabidopsis thaliana*. *Plant Cell* **19**: 1329–1346.
- Schwarz, C., Elles, I., Kortmann, J., Piotrowski, M., and Nickelsen, J.** (2007). Synthesis of the D2 protein of photosystem II in *Chlamydomonas* is controlled by a high molecular mass complex containing the RNA stabilization factor Nac2 and the translational activator RBP40. *Plant Cell* **19**: 3627–3639.
- Stampacchia, O., Girard-Bascou, J., Zanasco, J.L., Zerges, W., Bennoun, P., and Rochaix, J.-D.** (1997). A nuclear-encoded function essential for translation of the chloroplast *psaB* mRNA in *chlamydomonas*. *Plant Cell* **9**: 773–782.
- Steele, D.F., Butler, C.A., and Fox, T.D.** (1996). Expression of a recoded nuclear gene inserted into yeast mitochondrial DNA is limited by mRNA-specific translational activation. *Proc. Natl. Acad. Sci. USA* **93**: 5253–5257.
- Sturm, N.R., Kuras, R., Büschlen, S., Sakamoto, W., Kindle, K.L., Stern, D.B., and Wollman, F.A.** (1994). The *petD* gene is transcribed by functionally redundant promoters in *Chlamydomonas reinhardtii* chloroplasts. *Mol. Cell. Biol.* **14**: 6171–6179.
- Timmis, J.N., Ayliffe, M.A., Huang, C.Y., and Martin, W.** (2004). Endosymbiotic gene transfer: Organellar genomes forge eukaryotic chromosomes. *Nat. Rev. Genet.* **5**: 123–135.

- Trebitsh, T., Meiri, E., Ostersetzer, O., Adam, Z., and Danon, A. (2001). The protein disulfide isomerase-like RB60 is partitioned between stroma and thylakoids in *Chlamydomonas reinhardtii* chloroplasts. *J. Biol. Chem.* **276**: 4564–4569.
- Vaistij, F.E., Boudreau, E., Lemaire, S.D., Goldschmidt-Clermont, M., and Rochaix, J.-D. (2000b). Characterization of Mbb1, a nucleus-encoded tetratricopeptide-like repeat protein required for expression of the chloroplast *psbB/psbT/psbH* gene cluster in *Chlamydomonas reinhardtii*. *Proc. Natl. Acad. Sci. USA* **97**: 14813–14818.
- Vaistij, F.E., Goldschmidt-Clermont, M., Wostrikoff, K., and Rochaix, J.-D. (2000a). Stability determinants in the chloroplast *psbB/T/H* mRNAs of *Chlamydomonas reinhardtii*. *Plant J.* **21**: 469–482.
- Wostrikoff, K., Choquet, Y., Wollman, F.-A., and Girard-Bascou, J. (2001). TCA1, a single nuclear-encoded translational activator specific for *petA* mRNA in *Chlamydomonas reinhardtii* chloroplast. *Genetics* **159**: 119–132.
- Wostrikoff, K., Girard-Bascou, J., Wollman, F.-A., and Choquet, Y. (2004). Biogenesis of PSI involves a cascade of translational auto-regulation in the chloroplast of *Chlamydomonas*. *EMBO J.* **23**: 2696–2705.
- Xie, Z., Culler, D., Dreyfuss, B.W., Kuras, R., Wollman, F.-A., Girard-Bascou, J., and Merchant, S. (1998). Genetic analysis of chloroplast *c*-type cytochrome assembly in *Chlamydomonas reinhardtii*: One chloroplast locus and at least four nuclear loci are required for heme attachment. *Genetics* **148**: 681–692.
- Xu, F., Morin, C., Mitchell, G., Ackerley, C., and Robinson, B.H. (2004). The role of the LRPPRC (leucine-rich pentatricopeptide repeat cassette) gene in cytochrome oxidase assembly: Mutation causes lowered levels of *COX* (cytochrome *c* oxidase) *I* and *COX III* mRNA. *Biochem. J.* **382**: 331–336.
- Zerges, W., and Rochaix, J.-D. (1998). Low density membranes are associated with RNA-binding proteins and thylakoids in the chloroplast of *Chlamydomonas reinhardtii*. *J. Cell Biol.* **140**: 101–110.
- Zerges, W., Wang, S., and Rochaix, J.-D. (2002). Light activates binding of membrane proteins to chloroplast RNAs in *Chlamydomonas reinhardtii*. *Plant Mol. Biol.* **50**: 573–585.

The Nucleus-Encoded *trans*-Acting Factor MCA1 Plays a Critical Role in the Regulation of Cytochrome *f* Synthesis in *Chlamydomonas* Chloroplasts

Alix Boulouis, Cécile Raynaud, Sandrine Bujaldon, Aude Aznar, Francis-André Wollman and Yves Choquet

Plant Cell 2011;23;333-349; originally published online January 7, 2011;
DOI 10.1105/tpc.110.078170

This information is current as of April 5, 2011

| | |
|---------------------------------|---|
| Supplemental Data | http://www.plantcell.org/content/suppl/2010/12/13/tpc.110.078170.DC1.html |
| References | This article cites 69 articles, 29 of which can be accessed free at: http://www.plantcell.org/content/23/1/333.full.html#ref-list-1 |
| Permissions | https://www.copyright.com/ccc/openurl.do?sid=pd_hw1532298X&issn=1532298X&WT.mc_id=pd_hw1532298X |
| eTOCs | Sign up for eTOCs at: http://www.plantcell.org/cgi/alerts/ctmain |
| CiteTrack Alerts | Sign up for CiteTrack Alerts at: http://www.plantcell.org/cgi/alerts/ctmain |
| Subscription Information | Subscription Information for <i>The Plant Cell</i> and <i>Plant Physiology</i> is available at: http://www.aspb.org/publications/subscriptions.cfm |